Cyclical regulation of the insulin-like growth factor binding protein 3 gene in response to 1α,25-dihydroxyvitamin D_3

Jussi Ryynänen
M.Sc. Thesis
Biochemistry
Department of Biosciences
University of Kuopio
December 2009

ABSTRACT

Cyclical regulation of the *insulin-like growth factor binding protein 3* gene in response to 1α,25-dihydroxyvitamin D_3

UNIVERSITY OF KUOPIO, The Faculty of Natural and Environmental Sciences, Curriculum of Biosciences

RYYNÄNEN Jussi Pekka

Thesis for Master of Science degree

Supervisors Prof. Carsten Carlberg, Ph.D.

Marjo Malinen, Ph.D.

December 2009

Keywords: Gene regulation, IGFBP3, 1α,25$(OH)_2D_3$, Gemini, VDRE, chromatin

The gene *insulin-like growth factor binding protein 3 (IGFBP3)* has been previously shown to be a primary vitamin D_3 receptor (VDR) target containing three vitamin D_3 response elements (VDREs) in its promoter. It is up-regulated by the natural VDR ligand, 1α,25-dihydroxyvitamin D_3 (1α,25$(OH)_2D_3$), and is also a mediator for 1α,25$(OH)_2D_3$-mediated growth inhibition. In this study, non-malignant MCF-10A human mammary cells showed cyclical *IGFBP3* induction with 60 min periodicity after detailed time course stimulation with 1α,25$(OH)_2D_3$. Cycling of mRNA was the outcome from ligand-dependent VDR association to all VDREs and histone 4 acetylation of the proximal VDREs. Interestingly, these actions were not observed in response to treatment with the 1α,25$(OH)_2D_3$ analog Gemini, where *IGFBP3* mRNA expression was linear and more prominent. To study this process in more detail, gene expression profiles of every of the 11 *histone deacetylase (HDAC)* genes were measured after stimulation with both ligands. HDACs are important mediators for chromatin condensation and transcriptional repression and therefore they also play a role in transcriptional cycling. Interestingly, only the *HDAC4* and *HDAC6* genes responded to 1α,25$(OH)_2D_3$ treatment, while none of them to Gemini. In addition, transcriptional cycling was eliminated after combined mRNA silencing of both *HDAC4* and *HDAC6*. Furthermore, HDAC4 and HDAC6 showed cyclical association with VDREs in response to VDR ligands. In conclusion, 1α,25$(OH)_2D_3$ regulates *IGFBP3* expression in a cyclical fashion with cyclical recruitment of VDR, HDAC4 and HDAC6 to VDREs on *IGFBP3* promoter. Because Gemini has stronger interactions with VDR, it does not induce transcriptional cycling, which results in stable *IGFBP3* mRNA induction.

ACKNOWLEDGEMENTS

I am grateful to many people for the support I received while writing this thesis. This thesis was done during 2008 and 2009 at the University of Kuopio in the Department of Biosciences at the Biochemistry unit in the research group of Prof. Carsten Carlberg. I would like to thank my supervisors Dr. Marjo Malinen and Prof. Carsten Carlberg for invaluable advise and professional guidance. I would like to thank Docent Sami Väisänen for collaborating in this project. Special acknowledgement belongs to Maija for the technical support and cell culturing. A number of other people in our research group have supported me during this project and I am grateful to all of them for creating such a nice atmosphere in the lab and keeping up the team spirit. I would also like to thank my friends for all the social events we had, which kept studies and leisure time in a good balance.

Finally, I would like to thank Eveliina for her encouragement and understanding during the whole period of my thesis. I will never forget the endless support and help.

Kuopio 11.12.2009

Jussi Ryynänen

ABBREVIATIONS

$1\alpha,25(OH)_2D_3$	1α,25-dihydroxyvitamin D_3
$25(OH)D_3$	25-hydroxyvitamin D_3
ALS	acid-labile subunit
CDK	cyclin-dependent kinase
ChIP	chromatin immuno-precipitation
CoA	co-activator
CoR	co-repressor
CYP	cytochrome P450
CYP24A1	cytochrome P450, family 24, subfamily A, polypeptide 1 gene
CYP27A1	cytochrome P450, family 27, subfamily A, polypeptide 1 gene
CYP27B1	cytochrome P450, family 27, subfamily B, polypeptide 1 gene
DBD	DNA-binding domain
DBP	vitamin D-binding protein
DMEM	Dulbecco's modified Eagle's medium
DR	direct repeat
ER	everted repeat
FAM	6-carboxyfluorescein
FBS	fetal bovine serum
acH4	acetylated histone H4
HAT	histone acetyltransferase
HDAC	histone deacetylase
IGF	insulin-like growth factor
IGF-I	insulin-like growth factor-I
IGF-II	insulin-like growth factor-II
IGF-IR	type I insulin-like growth factor receptor
IGF-IIR	type II insulin-like growth factor receptor
IGFBP	insulin-like growth factor binding protein
IR	inverted repeat
LBD	ligand-binding domain
LBP	ligand-binding pocket
MS	multiple sclerosis

NR	nuclear receptor
PBS	phosphate buffered saline
PTH	parathyroid hormone
RA	rheumatoid arthritis
pRb	retinoblastoma protein
RE	response element
RPLP0	ribosomal protein, large, P0
RT-qPCR	real-time quantitative PCR
RXR	retinoid X receptor
siRNA	small inhibitory RNA
Th1	T helper type I
Th2	T helper type II
TSS	transcription start site
TGF-β	transforming growth factor-β
VDR	vitamin D_3 receptor
VDRE	vitamin D_3 response element

TABLE OF CONTENTS

1 INTRODUCTION

The pro-hormone vitamin D_3 is produced in skin or taken up from diet. It is converted in the liver and the kidneys to 1α,25-dihydroxyvitamin D_3 (1α,25$(OH)_2D_3$), which is the biologically active form of vitamin D_3 (Haussler *et al.,* 1998). The main role of 1α,25$(OH)_2D_3$ is in regulation of calcium and phosphate homeostasis and bone mineralization, but it also has important pro-apoptotic and anti-proliferative effects in regulation of cell growth (DeLuca, 2004). 1α,25$(OH)_2D_3$ mediates its effects on gene regulation by activating the vitamin D_3 receptor (VDR) (Sutton & MacDonald, 2003). Circulating 1α,25$(OH)_2D_3$ levels are tightly regulated, including the regulation of 1α,25$(OH)_2D_3$ synthesis and feedback-mediated degradation (Haussler *et al.,* 1998).

VDR is a member of the nuclear receptor (NR) superfamily and is the only mediator for genomic actions of 1α,25$(OH)_2D_3$. Binding of 1α,25$(OH)_2D_3$ activates VDR by inducing a conformational change of its ligand-binding domain (LBD). Ligand-activated VDR functions as a heterodimer with retinoid X receptor (RXR) and acts as a direct regulator of target gene expression by binding to vitamin D_3 response elements (VDREs) within the regulatory region of VDR target genes (Toell *et al.,* 2000). During transcriptional activation, ligand-activated VDR recruits co-activators (CoAs). While unliganded, VDR associates with co-repressors (CoRs) and histone deacetylases (HDACs) that are removing histone acetylation (Polly *et al.,* 2000). Generally, acetylation of histones mediates transcriptional activation through chromatin decondensation, while deacetylation mediates transcriptional repression through chromatin condensation (Wegel & Shaw, 2005). Transcription induced by NRs has recently been shown to be a cyclical process, where altering states of repressing, activation and initiation take place (Degenhardt *et al.,* 2009). This process regulates tightly the transcriptional process via cyclical control of mRNA synthesis.

Because therapeutic levels of 1α,25$(OH)_2D_3$ cause hypercalcemic toxicity, thousands of synthetic 1α,25$(OH)_2D_3$ analogs are designed to improve medically interesting features of 1α,25$(OH)_2D_3$ and to decrease calcemic toxicity (Carlberg & Mouriño, 2003). An interesting analog is Gemini, which is a strong VDR agonist carrying two side chains,

while vitamin D_3 has only one. In addition, Gemini can bind VDR in a two different conformations (Väisänen *et al.,* 2003; Molnár *et al.,* 2006). In one conformation Gemini acts as an agonist, but in another conformation as an inverse agonist.

In this study, detailed time course experiments showed cyclical induction of the *IGFBP3* gene in response to $1\alpha,25(OH)_2D_3$ stimulation, but not in response to Gemini. Transcriptional cycling resulted from cyclical recruitment of VDR on VDREs at the *IGFBP3* promoter. In addition, the genes *HDAC4* and *HDAC6* were up-regulated in a cyclical fashion with $1\alpha,25(OH)_2D_3$, but not with Gemini. Interestingly, cycling of *IGFBP3* expression was diminished, when *HDAC4* and *HDAC6* expressions were down-regulated by siRNAs. This observation establishes the significant roles of HDAC4 and HDAC6 for the cyclical regulation of VDR target gene expression induced by the natural ligand. In addition, HDAC4 and HDAC6 showed VDR-ligand induced association with VDRE regions. In conclusion, up-regulation of *IGFBP3* mRNA expression in response to $1\alpha,25(OH)_2D_3$ is an interactive process, where cyclical recruitment of VDR, HDAC4 and HDAC6 to VDRE-containing promoter regions results in a cyclical mRNA accumulation.

2 LITERATURE REVIEW

2.1 1α,25(OH)$_2$D$_3$

2.1.1 Vitamin D$_3$ metabolism

Vitamin D_3 is a fat-soluble pro-hormone and is produced in skin or taken up from diet. Pre-vitamin D_3 is produced in skin through UVB-irradiation of 7-dehydrocholesterol in a multi-step process. Additionally, vitamin D_3 can be taken up from diet, such as dairy products, fish or eggs, but natural dietary sources are the minor component compared to the production in skin (Hollis, 2005). Vitamin D_3 deficiency is very common and worldwide problem. The main reasons are that UVB radiation reduces towards northern latitudes and that skin pigmentation reduces vitamin D_3 production (Lips, 2006). In addition, personal and cultural behavior affects largely to UVB exposure. To prevent vitamin D_3 deficiency, vitamin D_3 is added to fortified milk products in many countries and different products of supplementary vitamin D_3 are commonly available for consumers.

Vitamin D_3 is hydroxylated by liver 25-hydroxylases, encoded by the cytochrome P450 (CYP) genes *CYP27A1* or *CYP2R1*, to 25-hydroxyvitamin D_3 (25(OH)D_3) that is an inactive form of vitamin D_3, and stored in the liver (Deeb *et al.,* 2007). In general, serum 25(OH)D_3 levels represents the whole body's vitamin D_3 status and low serum 25(OH)D_3 levels are a good marker of vitamin D_3 deficiency (Garland *et al.,* 2006). 25(OH)D_3 is subsequently hydroxylated mainly in kidneys to 1α,25(OH)$_2$D$_3$ by mitochondrial 1α-hydroxylase encoded by the gene *CYP27B1* (Haussler *et al.,* 1998). This active form of vitamin D_3 is the actual hormone and mediates most of the actions of all vitamin D_3 derivates. Both 1α,25(OH)$_2$D$_3$ and 25(OH)D_3 can be 24-hydroxylated to the metabolites 1α,24,25(OH)$_3$D$_3$ and 24,25(OH)$_2$D$_3$, respectively, which leads to catabolism of these metabolites. 24-hydroxylation is mediated by 25-hydroxyvitamin D_3 24-hydroxylase (24-OHase), encoded by gene *CYP24A1*. In the circulation, all vitamin D_3 metabolites are bound to vitamin D-binding protein (DBP), which binds with high affinity those metabolites and has a high homology to albumin (Lips, 2006). All metabolic steps are presented in Figure 1.

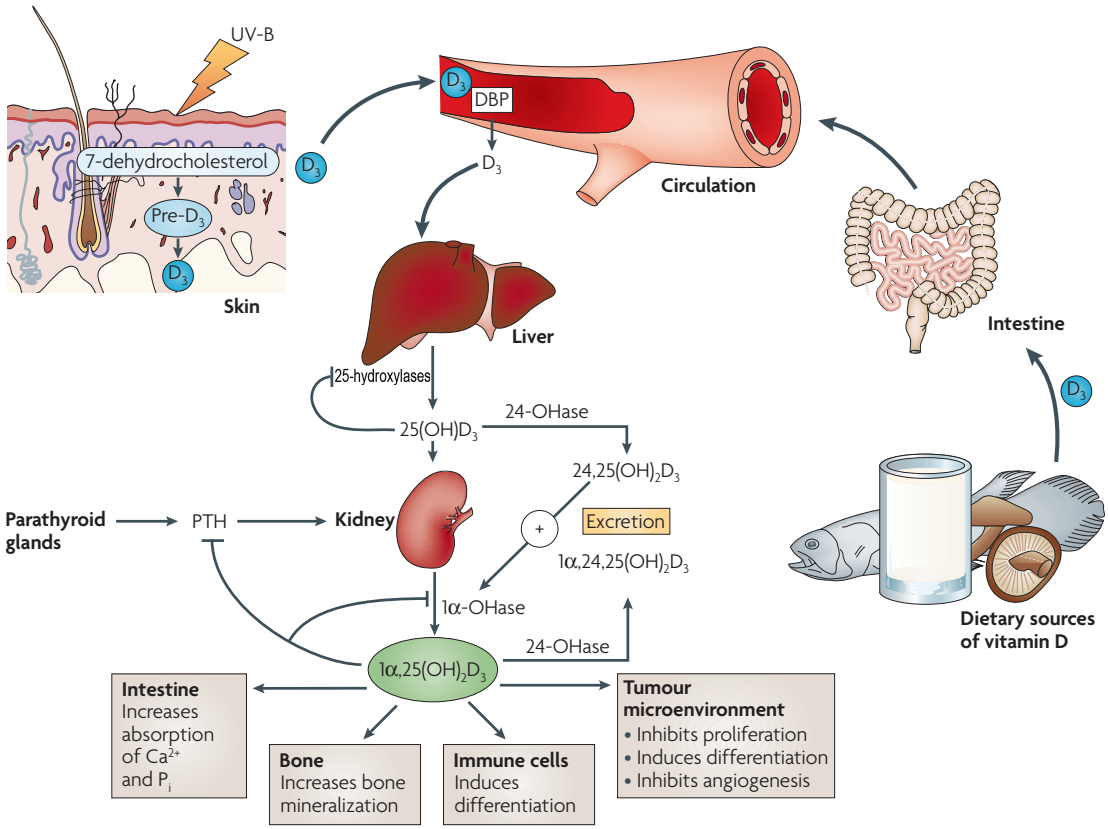

Figure 1. Vitamin D_3 metabolism (Adapted from Deeb *et al.,* 2007). Vitamin D_3 is produced in skin or obtained from diet. Circulating pre-vitamin D_3 is bound to DBP and is converted to the active metabolites, $25(OH)D_3$ and $1\alpha,25(OH)_2D_3$, by the liver and the kidneys. Parathyroid hormone (PTH) induces $1\alpha,25(OH)_2D_3$ production and 24-OHase mediates degradation of both $1\alpha,25(OH)_2D_3$ and $25(OH)D_3$.

The $1\alpha,25(OH)_2D_3$ metabolism is tightly regulated to maintain constant $1\alpha,25(OH)_2D_3$-levels. Parathyroid hormone (PTH) induces renal *CYP27B1* expression, which increases $1\alpha,25(OH)_2D_3$ production. In contrast, increasing levels of $1\alpha,25(OH)_2D_3$ repress *CYP27B1* expression and induce strongly *CYP24A1* expression, which mediates reduced production and increased degradation of active vitamin D_3 metabolites (Haussler *et al.,* 1998). There is also an extra-renal tissue-specific regulation of *CYP27B1* expression, which reveals both regulation and function of $1\alpha,25(OH)_2D_3$ metabolism in a tissue-specific manner (Zehnder *et al.,* 2001).

2.1.2 1α,25(OH)$_2$D$_3$ actions on bone

An important role of 1α,25(OH)$_2$D$_3$ is in regulation of calcium and phosphate homeostasis and of bone mineralization (DeLuca, 2004; Lips, 2006). It is the only known hormone that directly induces i) production of proteins being involved in active intestinal calcium intake and ii) intestinal phosphate absorption (Wasserman & Fullmer, 1995; DeLuca, 2004). PTH production is actively induced in response to decreased calcium levels, which leads to production of more 1α,25(OH)$_2$D$_3$ and thus increased calcium levels. In cases when environmental calcium is not sufficiently available, both 1α,25(OH)$_2$D$_3$ and PTH induce bone resorption and reduce renal calcium excretion to maintain adequate serum calcium level (Suda *et al.,* 2002). In contrast, increased calcium levels decrease PTH production and activate osteoblast formation in the bone. Overall, this regulatory network maintains both calcium and 1α,25(OH)$_2$D$_3$ levels in balance, which in turn keeps the formation and resorption of bone in balance. In vitamin D$_3$ deficiency or in cases when 1α,25(OH)$_2$D$_3$ metabolic pathways (such the *CYP27B1* gene) are inoperative, calcium resorption from bone is increased due to the reduced intestinal intake and increased PTH levels, which can lead to osteomalacia or rickets (Lips, 2006).

2.1.3 Anti-tumor actions of 1α,25(OH)$_2$D$_3$

In addition to its role in mineral metabolism, it has been shown that 1α,25(OH)$_2$D$_3$ also plays important role in cell growth regulation and has anti-proliferative features (Ingraham *et al.,* 2008). Furthermore, several epidemiological studies and meta-analyses have shown that low serum 25(OH)D$_3$ levels are connected to increased cancer incidents of the breast, colon, prostate and ovary and it is believed that adequate levels, in contrast, would offer a protective role against these cancers (Ingraham *et al.,* 2008; Garland *et al.,* 2006). In addition, overexpression of the *CYP24A1* gene has been reported in several type of cancer tissues, which leads to reduced anti-cancer effects of 1α,25(OH)$_2$D$_3$ (Deeb *et al.,* 2007).

In breast cancer cells the anti-cancer action of 1α,25(OH)$_2$D$_3$ includes cell cycle arrest and induction of apoptosis and differentiation (Welsh, 2007a; Mathiasen *et al.,* 1999; Verlinden *et al.,* 1998). However, these anti-cancer features vary between different cell and cancer types. In MCF-7 human breast cancer cells 1α,25(OH)$_2$D$_3$ can induce

retinoblastoma protein (pRb)-mediated G_1/G_0 cell cycle arrest by up-regulating gene expression of the cyclin-dependent kinase (CDK) inhibitor genes *CDKN1A* and *CDKN1B* which encode protein p21 and p27 respectively (Verlinden *et al.,* 1998). This leads to inhibition of CDK activity, which in turn causes pRb hypophosphorylation and pRb-mediated cell cycle arrest.

In addition to its capacity to induce cell cycle arrest, $1\alpha,25(OH)_2D_3$ is able to induce apoptosis in MCF-7 and T47D cells (Mathiasen *et al.,* 1999). Apoptosis is caused by down-regulation of the anti-apoptotic protein Bcl-2 and by translocation of the pro-apoptotic protein Bax from the cytosol to mitochondria in response to $1\alpha,25(OH)_2D_3$ treatment. However, overexpression of Bcl-2 is able to prevent this $1\alpha,25(OH)_2D_3$-induced apoptosis, which suggests the involvement of the Blc-2 pathway in this process. Moreover, Xie *et al.* (1999) found that in these cell lines $1\alpha,25(OH)_2D_3$ induces growth inhibition by down-regulation of the insulin-like growth factor (IGF) signaling pathway, which leads to promotion of apoptosis. IGFs are strong anti-apoptotic peptides that mediate their mitogenic signals mainly through type I IGF receptor (IGF-IR) (Hwa *et al.,* 1999). In addition, overexpression of IGF-IR is one feature of breast cancer cell and high levels of circulating IGFs are strongly associated to breast cancer risk (Renehan *et al.,* 2006). Furthermore, up-regulation of proteins that are involved in regulating the actions of IGFs, such as IGFBPs, is one feature of $1\alpha,25(OH)_2D_3$-mediated growth inhibition in breast cancer cells (Colston *et al.,* 1998). IGFBPs will be discussed in more detailed in chapter 2.4.

However, anti-cancer effects of $1\alpha,25(OH)_2D_3$ do not limit only to growth inhibition of cancer cells, but $1\alpha,25(OH)_2D_3$ signaling has also been associated in preventing carcinogenesis. $1\alpha,25(OH)_2D_3$ directly regulates key proteins involved in proliferation and differentiation of normal mammary cells (Welsh, 2007b). In the mouse mammary gland, the VDR is localized mainly in differentiated cells. During pregnancy and lactation, when cells undergo differentiation, expression of VDR is increased about 100-fold, while VDR knockout mice are undergoing excessive proliferation and impaired apoptosis (Zinser *et al.,* 2002; Zinser & Welsh, 2004). In general, $1\alpha,25(OH)_2D_3$ signaling is found to promote or maintain the differentiated phenotype of normal mammary cells and also animal models have shown that $1\alpha,25(OH)_2D_3$ signaling protects against carcinogenesis of mammary cells

(Welsh, 2007a). In addition, several epidemiological studies are consistent with the protective role of 1α,25$(OH)_2D_3$ in carcinogenesis (Deeb *et al.,* 2007).

2.1.4 1α,25$(OH)_2D_3$ actions on immunity

1α,25$(OH)_2D_3$ signaling has been shown to have potent immunomodulatory effects in both innate and adaptive immune cells (Nagpal *et al.,* 2005). VDR is expressed and is inducible by 1α,25$(OH)_2D_3$ in central immune cells, such as T-cells, monocytes/macrophages and natural killer cells (Veldman *et al.,* 2000). In addition, several epidemiological studies have shown reduced serum 25$(OH)D_3$ levels in autoimmune diseases such as multiple sclerosis (MS), type I diabetes and rheumatoid arthritis (RA) (Nagpal *et al.,* 2005). Adequate serum 25$(OH)D_3$ level, especially earlier in life, is suggested to offer protection against multiple sclerosis (Munger *et al.,* 2006). Furthermore, VDR-ligands have shown to directly inhibit production of IL-12 cytokines by monocytes, which, in turn, leads to reduced T helper I (Th1) development without affecting T helper II (Th2) development (Mattner *et al.,* 2000). Th1 cells play central role in MS, and reduction of Th1 development has been shown to be beneficial in treatment of MS in animal models.

Administration of 1α,25$(OH)_2D_3$ has been shown to be protective also in other autoimmune diseases. In NOD mice, which are the most widely used animal model for type I diabetes, onset of type I diabetes could be prevented by 1α,25$(OH)_2D_3$ and its synthetic analog administration (Mathieu *et al.,* 1994, 1995). In addition, human study with high 1α,25$(OH)_2D_3$ administration from 1-year of age resulted in 80 % decreased risk of developing type I diabetes later in life (Hyppönen *et al.,* 2001). Synthetic 1α,25$(OH)_2D_3$ analogs also effectively inhibited progression of ongoing type I diabetes in NOD mice (Gregori *et al.,* 2002). This inhibition was associated with reduced Th1 infiltration into the pancreas, which was consequence from reduced IL-12 production. Furthermore, 1α,25$(OH)_2D_3$ or analog administration promoted improvement in RA symptoms and disease activity (Andjelkovic *et al.,* 1999). All these features establish that 1α,25$(OH)_2D_3$, has an important role in the immune system by mediating Th1 suppression and adequate 1α,25$(OH)_2D_3$ intake may also reduce incidents of central autoimmune diseases.

2.2 Vitamin D_3 receptor

2.2.1 Overview of nuclear receptors

The VDR belongs to the 48-member superfamily of nuclear receptors (NRs) that are ligand-activated transcription factors and regulate gene expression of target proteins involved in various processes such as metabolism, reproduction and development (McKenna & O'Malley, 2002). In addition, VDR is one of the members of the classic 12 nuclear receptors that function as endocrine receptors, which bind their ligands with high affinity (Chawla *et al.,* 2001) Ligands for NRs can be involved in endocrine signaling, such as thyroid and steroid hormones, or lipids involved in fatty acid metabolism (Li *et al.,* 2003). There is also a group of orphan receptors, which ligands are either unknown or they are not ligand-activated at all (Benoit *et al.,* 2006). Because NRs are central regulators of various genes, they serve as a good drug targets for numerous diseases such as asthma, type 2 diabetes, atherosclerosis and cancer. Structurally NRs share a highly conserved DNA-binding domain (DBD) and a structurally conserved carboxy-terminal ligand-binding domain (LBD) (Carlberg & Molnár, 2006). The DBD contains two conserved zinc finger motifs, which bind to specific DNA sequences, known as response elements (RE), in a regulatory region of target gene, while LBD contains a ligand-binding pocket (LBP), which serves as a binding site for the receptor-specific ligand (Chawla *et al.,* 2001, Carlberg & Molnár, 2006). In general, NRs can be considered as molecular switches for transcription of those genes that contain response element in their promoter region (Carlberg & Polly, 1998).

2.2.2 VDR function

VDR is the only mediator of the genomic actions of $1\alpha,25(OH)_2D_3$, is expressed widely and can be detected in all human tissues (Carlberg, 2004; Carlberg *et al.,* 2007). Primary $1\alpha,25(OH)_2D_3$ target genes contain usually several $1\alpha,25(OH)_2D_3$ response elements (VDREs), which are formed by two hexameric DNA sequences, core-binding motif, with the consensus sequence RGKTSA (R = A or G, K = G or T, S = C or G) (Carlberg & Polly, 1998). Furthermore, core-binding motifs can be organized in three different

configurations; direct repeat (DR), everted repeat (ER) and inverted repeat (IR), with few intervening nucleotides. VDR regulates transcription by binding directly to VDREs primary as a heterodimer with RXR (Toell *et al.,* 2000). VDR-RXR heterodimers prefer binding to DR-type motifs with 3 intervening nucleotides known as DR3 (Umesono *et al.,* 1991). However, this is not the only functional VDRE motif and other functional VDRE-motifs are reported, such as DR4, ER6, ER7, ER8 and ER9 (Schräder *et al.,* 1995; Quack & Carlberg, 2000). In addition, VDREs can be located on both DNA strands and also far away from transcription start site (TSS). For example, *IGFBP3* promoter contains a tandem of two VDREs at position -400 and another VDRE in another strand at position -3350 relative to TSS (Peng *et al.,* 2004; Matilainen *et al.,* 2005).

When unliganded, VDRE-bound VDR-RXR-dimers associate with nuclear co-repressor proteins (CoRs), such as NCoR and SMRT, which in turn associate with histone deacetylases (HDACs) and keep chromatin in locally condensed and transcriptionally repressed state (Polly *et al.,* 2000). Binding of $1\alpha,25(OH)_2D_3$ to the LBP of LBD changes the conformation of LBD, which destabilizes the CoR-VDR complex and results in release of CoRs and subsequent recruitment of co-activator (CoA) proteins, such as proteins of the p160-family (Leo & Chen, 2000). Some CoAs have histone acetyltransferase (HAT) activity or are complexed with proteins having such activity and this results in local chromatin decondensation (Castillo *et al.,* 1999). Ligand-activated VDR subsequently releases CoAs of the p160 family and interacts with those CoAs of mediator complexes, such as Med1 (Rachez *et al.,* 1998). The mediator complex is a multi-subunit CoA complex and consist of 15-20 proteins, which build a bridge between VDR and basal transcription machinery located on the TSS (Rachez *et al.,* 1999). Through these events $1\alpha,25(OH)_2D_3$-activated VDR can mediate both the modification of chromatin and direct regulation of transcription by protein-protein interactions. These ligand-induced actions of VDR are in central role in nuclear $1\alpha,25(OH)_2D_3$ signaling and activation of transcription.

As described, transcription mediated by NRs is a dynamic process. In addition, recent chromatin immunoprecipitation (ChIP) and mRNA expression studies have shown both cyclical promoter activation and mRNA expression mediated by NRs, such as estrogen receptor α on the *trefoil factor-1* gene, peroxisome proliferater-activated receptor δ on the *pyryvate dehydrogenase kinase 4* gene and VDR on the *CYP24A1* and *CDKN1A* genes (Métivier *et al.,* 2003; Kim *et al.,* 2005; Degenhardt *et al.,* 2009; Saramäki *et al.,* 2009).

According to these studies, dynamic nature of transcription is a tightly regulated cyclical process, where alternating activation and repression takes place.

2.2.3 1α,25(OH)$_2$D$_3$ analogs as VDR ligands

It is well established that 1α,25(OH)$_2$D$_3$-activated VDR possesses many potential therapeutic features and is therefore a very interesting target for medical applications. However, several clinical trials with 1α,25(OH)$_2$D$_3$ have been failed because of the hypercalcemic toxicity of the hormone (Deeb *et al.,* 2007). Therefore over 3000 1α,25(OH)$_2$D$_3$ analogs have been designed over the years in order to prevent hypercalcemia and to improve biological capacity of the natural hormone in hyper-proliferative diseases, such as cancer, or in bone disorders, such as osteoporosis (Bouillon *et al.,* 1995; Carlberg & Mouriño, 2003). Most of the analogs carry a modification in their side chain, which in many cases also declines their 24-OHase-mediated degradation and increases stability of the VDR-ligand complex (van den Bemd *et al.,* 1996; Bury *et al.,* 2001). In addition, many analogs have either low or sometimes extremely low affinity to DBP (Bouillon *et al.,* 1996). Low DBP binding and altered intracellular metabolism of analogs compared to natural ligand creates also distinctive tissue-specific pharmacokinetic features for VDR ligands.

Most of the 1α,25(OH)$_2$D$_3$ analogs are agonists and only few are identified as antagonists. An interesting analog is Gemini, which has two identical side chains (Figure 2) and has therefore a 20% bigger volume than natural ligand (Herdick *et al.,* 2000; Norman *et al.,* 2000). Despite the size of Gemini, the LBP of the VDR is flexible enough to accommodate Gemini in two different conformations (Väisänen *et al.,* 2003; Molnár *et al.,* 2006). As one of the side chains takes the same position as that of natural ligand, Gemini acts as an agonist. In contrast, Gemini can act as an inverse agonist, when both side chains take alternative position to that of natural hormone (Gonzales *et al.,* 2003). Further changes between agonistic and inverse agonistic conformations were found to response in cellular CoA and CoR levels. In normal or CoA-rich circumstances Gemini acts as an agonist and stabilizes VDR into active conformation, but at CoR excess Gemini can bind the LBP in inverse agonistic conformation, actively recruits CoRs to the VDR and induces repression. These features suggest that Gemini can sense the CoA/CoR ratio, which is an important

cell-specific characteristic. Taken together, 1α,25(OH)$_2$D$_3$ analogs have improved biological properties compared to that of the natural ligand without having hypercalcemic side effects and are therefore of great interest in research due to their potential for different type of therapeutic applications.

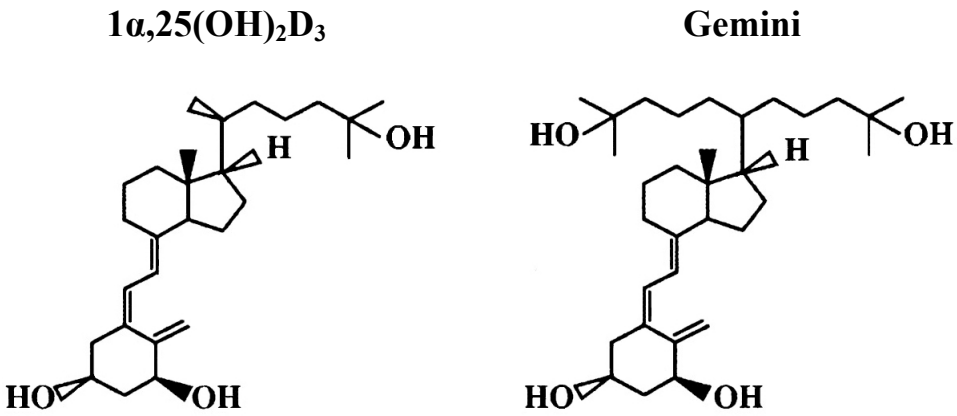

Figure 2. Molecular structure of 1α,25(OH)$_2$D$_3$ and Gemini. Gemini differs from 1α,25(OH)$_2$D$_3$ by having two identical side chain branching from carbon 20, while 1α,25(OH)$_2$D$_3$ has only one.

2.3 Chromatin structure

In every human cell there is almost 2 m of DNA-helix packed into the nucleus of about 10 µm diameter. This can be achieved only by tight organization of DNA into a complex with histone-proteins to form nucleosomes (Figure 3). In one nucleosome 145-147 bp of DNA-helix with a diameter of 2 nm is wrapped in 1.75 turns around a globular histone octamer to form a nucleosome core (Luger *et al.,* 1997). Core nucleosomes are separated by 10 to 90 bp of intervening linker-DNA. This forms chromatin structure that is considered as a 10 nm fibre or "bead on a string" conformation and is about 5- to 10-fold condensed (Felsenfeld & Groudine, 2003). The histone octamer is built from two subunits of each histone proteins, H2A, H2B, H3 and H4, which consist of a C-terminal histone fold domain and N-terminal tail domain (Hansen, 2002; Horn & Peterson, 2002). Histone fold domains form the actual core of the nucleosome with histone-histone and histone-DNA interactions, while tail domains are point outside from core nucleosome and serve as sites for posttranslational modifications (Luger *et al.,* 1997; Hansen, 2002; Horn & Peterson,

2002). In addition, histone tails are able to associate with linker-DNA or with adjacent nucleotides.

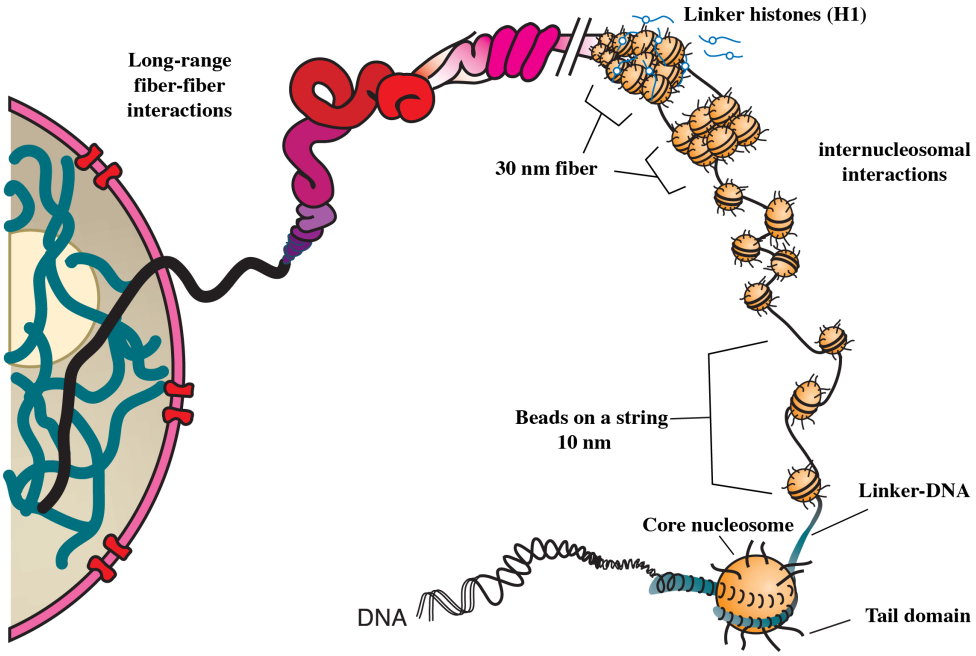

Figure 3. Structure of multiple levels of chromatin condensation (Adapted from Horn & Peterson, 2002). Histone octamers and wrapped DNA-strand form core nucleosomes and 10 nm DNA fiber by internucleosomal interactions. Histone H1 stabilizes the next condensation level, 30 nm fiber, which can be further condensed by fibre-fibre interactions.

Furthermore, the 10 nm fibre can be folded into a fibre with a diameter of about 30 nm producing a net compaction about 50-fold. This 30 nm fibre is stabilized by the linker-protein, histone H1, which binds the core nucleosome and linker-DNA to condense the structure even more (Felsenfeld & Groudine, 2003). In further condensation, the 30 nm fibre is through long-range fibre-fibre interactions folded into higher order structures. There are several models how chromatin is packed in higher condensation rates, but detailed structures and compaction rates remain still unknown (Horn & Peterson, 2002). In addition, the diameter of higher compaction of chromatin folding is observed to vary from 80 nm to several hundred nanometers (Horn & Peterson, 2002; Felsenfeld & Groudine, 2003).

Transcription requires group of enzymes, transcription factors and cofactors to either directly access into the chromatin or to the proteins associated with chromatin. Therefore

chromatin is static and highly packed only during the metaphase of mitosis, while interphase chromatin is very dynamic and in constant change between condensing and decondensing states (Wegel & Shaw, 2005). Chromatin is decondensed during gene activation and is condensed, when genes are silenced. When chromatin is decondensed, also referred as open chromatin, it is accessible for NRs and other components of the transcription machinery (Elgin & Grewal, 2003; Wegel & Shaw, 2005). In addition, gene-rich areas of chromosomes are usually observed as very heterogeneous open chromatin, while repetitive units and gene-poor areas of chromatin, such as centromers and telomers, are usually condensed (closed chromatin) and not accessible for the transcription machinery. However, open chromatin does not always mean transcriptional activity and it has been shown that gene-rich open chromatin can also be transcriptionally inactive (Gilbert *et al.,* 2004). In contrast, gene can be active in a gene-poor and largely condensed chromatin area, if there is enough local decondensation to open chromatin for transcription machinery. Therefore, it is suggested that open chromatin is required for transcription, but does not always stand for it.

The central mechanisms for modifying higher order of chromatin folding are posttranslational modifications of amino acid residues of the histone tails, such as lysine acetylation, lysine or arginine methylation and serine phosphorylation (Spotswood & Turner, 2002). In addition, histones can be modified by adding small peptides, such as ubiquitin or ubiquitin-like proteins (Gill, 2004). These posttranslational modifications of histone tails are reversible and in every histone type there are several possible positions for different modifications. When put together, these modifications form a large complex of different combinations. In addition, within the genomic region of one gene there can be several hundreds of nucleosomes. Different combinations of modifications can efficiently affect chromatin condensation and transcriptional regulation in a combination-dependent manner and thus it is suggested that histone tail modification patterns can contain epigenetic information, called the histone code (Jenuwein & Allis, 2001; Turner, 2002). Furthermore, once chromatin is opened, the next level of chromatin modification can be achieved through ATP-dependent nucleosome remodelling that was first observed *in vitro* in *Drosophila* embryo extracts (Varga-Weisz *et al.,* 1995). With nucleosome remodelling, accessibility of DNA is increased even more by stripping DNA from nucleosomes through energy-dependent relocation, reassembling and sliding of histone octamers (Becker, 2002).

2.3.1 Histone acetylation and deacetylation

Probably the best understood type of histone modification is acetylation of the lysine residues in core histone tails, which is executed by enzymes with HAT activity. Generally, histone acetylation is connected to gene activity through local chromatin decondensation, while decreased acetylation levels are associated with transcriptional repression. Acetylation of histones neutralizes positive charges of lysine residues and decreases their affinity to DNA, which in turn increases accessibility of transcription factors to DNA (Grunstein, 1997). However, histone acetylation does not limit only to the regulation of transcription, since there is also group of HAT proteins that are located in cytoplasm and are acetylating newly synthesized histones to assemble them as already acetylated into chromatin (Brownell, 1996). In addition, removing of acetyl groups is mediated by HDACs, which mediate chromatin condensation. NRs can interact with HDACs via CoRs whereas many CoAs possess HAT activity (Castillo *et al.,* 1999; Polly *et al.,* 2000). Therefore, histone acetylation is general part of NR-mediated transcription.

HDACs are a 18-member group of proteins consisting of two protein families with HDAC activity; the classic HDAC family (HDACs 1-11) and sirtuin family (SIRTs 1-7). These proteins can be further divided into four different classes (Table 1). HDACs do not bind directly to DNA and are usually part of a large multi-protein complex (Verdin *et al.,* 2003). Class I HDACs are found almost exclusively in the nucleus, are ubiquitously expressed and seem to be involved in general cellular processes (Verdin *et al.,* 2003; Gregoretti *et al.,* 2004). In addition, HDAC3 can stably associate with the CoRs SMRT and NCoR to form multi-protein repressor complex.

In contrast to Class I, HDACs of Class II are able to shuttle between nucleus and cytoplasm in response to cellular signals and their mRNA expression is tissue specific. Class II can be further divided in two subgroups (IIa and IIb) based on their domain organization and sequence homology (Verdin *et al.,* 2003). Furthermore, Class IIa HDACs 4, 5 and 7, having rather low deacetylase activity, are able to mediate their deacetylation by association directly with SMRT/NCOR-complex, which is a part of a multi-protein complex containing HDAC3 (Fischle, 2001; 2002). Without HDAC3 this complex is inactive, which suggest that HDAC3 brings enzymatic activity to that stable complex, while HDAC4, 5 and 7 can regulate this complex by recruiting it to gene promoters.

HDAC11, that forms alone the Class IV, is found primarily in nucleus. It is evolutionally related to HDAC3 and HDAC8, but it is not found from any known HDAC complexes, which suggest that it has biochemically distinct function (de Rujiter *et al.,* 2003). Furthermore, sirtuins, that form Class III, are related to the yeast Sir2 protein and are also found in multi-protein complexes. All sirtuins are NAD-dependent deacetylases, while all other HDACs, in contrast, require zinc ion as a substrate into charge-relay deacetylation activity. In general, HDACs are important mediators of deacetylation and act as components of diverse repressor complexes.

Table 1. HDACs can be divided in four classes. HDACs 1, 2, 3 and 8 forms Class I. Class II can be divided in two subgroups, of which group a consists of HDACs 4, 5, 7 and 9, while HDACs 6 and 10 belong to group b. All 7 sirtuins form Class III and HDAC11 alone makes up Class IV.

Class I	HDAC1, HDAC2, HDAC3, HDAC8
Class IIa	HDAC4, HDAC5, HDAC7, HDAC9
Class IIb	HDAC6, HDAC10
Class III	SIRT1-7
Class IV	HDAC11

2.4 IGFBP3

2.4.1 IGFBP3 as a modulator of IGF signaling

IGFBPs are a family of proteins that regulate IGF-system by binding IGFs with high affinity. There are six well-identified mammalian IGFBPs, named IGFBP1 through IGFBP6, that are produced mainly by hepatic cells (Hwa *et al.,* 1999; Zimmermann *et al.,* 2000). The IGF system is the mediator for cellular mitogenic signals; its role in cell growth and differentiation is well established. The system consists of circulating IGF-I and IGF-II, which mediate their growth signals in target tissues through cell surface receptors, type I and II IGF-receptors (IGF-IR and IGF-IIR) or insulin receptor. Both IGFs (IGF-I and IGF-II) are mediating their mitotic signals mainly by binding and activating the IGF-IR (Hwa *et al.,* 1999). Most of the IGFs are produced by hepatocytes in response to growth hormone stimulation and subsequently secreted to circulation to mediate mitogenic signals in target tissues (Zimmermann *et al.,* 2000).

In circulation, IGFs (sized about 7 kDa) are rapidly degraded with a half-life of roughly 10 min (Baxter, 1994). To stabilize IGFs, over 90 % are bound to ternary complex, composed of one molecule of each IGF, acid-labile subunit (ALS) and IGFBP3, with total size of 150 kDa. In the complex, IGF's half-life is found to increase up to 15 h (Guler *et al.,* 1989). Interestingly, IGFBPs bind to IGFs with higher affinity than IGFs bind to their receptors and therefore IGFBP3, as a main binder of IGFs, is not only carrier and stabilizer of IGFs but is also able to regulate its bioavailability and signaling through IGF-Rs (Hwa *et al.,* 1999). Moreover, a study performed with promyeloid HL-60 and monocytic U-937 cell lines has shown that IGFBP3 is able to suppress IGF-induced proliferation in these cells, while des-(1-3)-IGF-I, an IGF-I analog that does not bind to IGFBP3, stimulated cell proliferation (Li *et al.,* 1997). In addition, membrane-associated IGFBP3 attenuates IGF-I-induced IGF-IR signaling in endometrial cancer cells overexpressing both IGF-IR and membrane-bound IGFBP3, while des-(1-3)-IGF-I caused receptor activation (Karas *et al.,* 1997). In contrast, the same study showed that fibroblast cells lacking membrane-bound IGFBP3 but overexpressing IGF-IR showed similar IGF-IR activation to IGF-I and des-(1-3)-IGF-I. These findings establish that IGFBP3 has significant growth-inhibitory effects by preventing IGF-I binding to IGF-Rs.

Most of the circulating IGFBP3 is produced by hepatic Kupffer cells and endothelial cells to assemble them into the IGF-ALS-IGFBP3 complex or to secrete to circulation. However, IGFBP3 is produced also in a tissue-specific manner to mediate auto- and paracrine growth regulation (Yamada & Lee, 2009). In addition, *IGFBP3* expression is found to be inducible by several growth inhibition agents, such as $1\alpha,25(OH)_2D_3$, transforming growth factor-β (TGF-β), TNF-α and retinoic acid in various cancer cell types, such as breast, prostate and fibroblast cancer cells. The *IGFBP3* gene is a primary $1\alpha,25(OH)_2D_3$ target and has three response elements in its promoter (Figure 5, page 37), of which first two are located as tandem at position -400 bp (RE1/2) and third at position -3350 bp (RE3) (Matilainen *et al.,* 2005). Rat prostate *in vivo* and prostate cancer *in vitro* studies with $1\alpha,25(OH)_2D_3$ and its analogs have shown that ligand treatment induces *IGFBP3* expression, which leads to decreased cell proliferation (Nickerson & Huynh, 1999). This locally induced *IGFBP3* is suggested to decrease IGFs availability and hence inhibit prostate or cell growth. Growth inhibition of MCF-7 and Hs578T human breast cancer cells induced by $1\alpha,25(OH)_2D_3$ was also associated with increased *IGFBP3* expression (Colston *et al.,* 1998). Furthermore, during p53-mediated apoptosis of colon carcinoma cells, p53 was directly found to up-regulate *IGFBP3* expression via two p53 response elements found in *IGFBP3* introns (Buckbinder *et al.,* 1995).

2.4.2 IGF-independent actions of IGFBP3

Circulating or locally produced IGFBP3 is also able to mediate IGF-independent growth inhibition signaling. In addition, induction of *IGFBP3* expression is a central tool studying IGF-independent actions in different cell types. It is suggested that IGFBP3 mediates its growth signaling actions through specific cell surface receptor, but to date, the specific receptor has not been published (Yamada & Lee, 2009). There are two putative receptors; firstly, Leal *et al.* (1997) found that in mink lung epithelial cells IGFBP3 binds to TGF-β type V receptor, but detailed signaling mechanism remains unknown. Secondly, Yamanaka *et al.* (1999) found that IGFBP3 to binds unknown receptor in breast cancer cell surface. Signaling of the receptor remains unknown, but it was found to bind IGFBP3 with high affinity and specificity. In addition, IGFBP3 contains a nuclear localization signal in its sequence and it has been shown to localize in nucleus (Jacques *et al.,* 1997; Schedlich *et*

al., 1998). In the nucleus, IGFBP3 is able to directly control transcription by binding to RXRα (Liu *et al.,* 2000). RXRα is also required for IGFBP3-mediated apoptosis. Furthermore, it has been shown that IGFBP3 stimulates RXR-α-Nur77-heterodimers to translocate from the nucleus into mitochondria, which initiates caspase activation and apoptosis (Lee *et al.,* 2005).

However, IGFBP3 is able to mediate its growth inhibitive actions without binding to the cell surface or localizing into the nucleus. Increased *IGFBP3* expression was shown to lead caspase-mediated apoptosis with reduced IGFBP3 cell surface binding and without localization into nucleus in study performed with T47D breast cancer cells (Butt *et al.,* 2002). In LNCaP prostate cancer cells IGFBP3 induced by $1\alpha,25(OH)_2D_3$ was found to be critical for induction of *CDKN1A* expression and growth inhibition mediated by its gene product, p21 (Boyle *et al.,* 2001). When IGFBP3 was withdrawn, no growth inhibition or *CDKN1A* expression was observed in response to $1\alpha,25(OH)_2D_3$. In contrast, a previous prostate cancer study (Nickerson & Huynh, 1999) suggested that $1\alpha,25(OH)_2D_3$ and its analogs induce IGFBP3-mediated but IGF-dependent growth inhibition. These findings establish that there are several pathways for IGFBP3 to inhibit cell growth and these pathways may be also cell-type specific.

3 AIMS OF THE STUDY

This study aims to investigate VDR-mediated regulation of the *IGFBP3* gene by using two different VDR ligands; 1α,25$(OH)_2D_3$ and Gemini. More specific aims are:

1. To study the effects of 1α,25$(OH)_2D_3$ and Gemini treatment on *IGFBP3* mRNA accumulation in MCF-10A cells by using real-time quantitative (RT-q) PCR.

2. To monitor the ligand-mediated changes in VDR binding and histone 4 acetylation level at VDREs in *IGFBP3* promoter by using ChIP assays.

3. To study the role of HDACs in *IGFBP3* mRNA accumulation induced by VDR ligands.

4 MATERIALS AND METHODS

4.1 Cell culture

All experiments in this thesis were done with MCF-10A cells. The human mammary epithelial cell line MCF-10A is an estrogen receptor negative and non-tumorigenic immortalized cell line. MCF-10A were grown in a mixture of phenol red-free Dulbecco's modified Eagle's medium (DMEM) and Ham's F12 medium (1:1) with 20 ng/ml of epidermal growth factor, 100 ng/ml of cholera toxin, 10 µg/ml insulin, 500 ng/ml hydrocortisone, 0.1 mg/ml streptomycin, 100 U/ml penicillin and 5% horse serum. Cells were grown in humidified 95% air / 5% CO_2 incubator at 37 °C.

For mRNA and ChIP experiments the cells were seeded in the above-mentioned medium but with 5% charcoal-stripped fetal bovine serum (FBS) instead of horse serum. FBS was stripped of lipophilic compounds by stirring it with 5% (w/v) activated charcoal (Sigma-Aldrich) for 3 h at room temperature. Charcoal was then removed by centrifugation and sterile filtration (0.2 mm pore size). The cells were grown for 24 h to reach a density of 50 to 60% confluence.

During experiments, the cells were treated with either EtOH (0.001%), $1\alpha,25(OH)_2D_3$ or Gemini (both ligands were kindly provided by Dr. Milan Uskokovic, BioXell Inc., Nutley, NJ, USA). $1\alpha,25(OH)_2D_3$ and Gemini were used at a final concentration of 10 nM diluted in DMEM with 0.001% EtOH. All treatments were done without refreshing the medium.

4.2 RNA extraction and cDNA synthesis

Cells were seeded into 6-well plates and grown 24 h before ligand treatment. The cells were stimulated with ligands for indicated time periods. Total RNA was isolated from the cells using High Pure RNA Isolation Kit (Roche Diagnostic, Mannheim, Germany) as instructed by the manufacturer. Lysis of the cells was performed by adding 200 µl phosphate buffered saline (PBS; 150 mM NaCl, 2 mM KCl, 1.5 mM KH_2PO_4, 10 mM Na_2HPO_4 x H_2O) and 400 µl lysis buffer directly on culture plate after washing cells once

with PBS. Final elution of RNA was done in 50 μl of elution buffer. Total RNA amount and purity was quantified with a NanoDrop ND-1000 spectrophotometer (NanoDrop, Wilmington, DE, USA)

cDNA synthesis was performed using the Transcriptor First Strand cDNA synthesis kit (Roche, Mannheim, Germany) as instructed by the manufacturer. Template RNA (1 μg) was pre-incubated for 10 min with 50 pmol oligo$(dT)_{18}$ primer at 65 °C to denature secondary structures of RNA. Oligo$(dT)_{18}$ primers anneal to poly-A tail of mRNA. The synthesis was performed for 30 min at 55 °C in a total volume of 20 μl. After synthesis, the reaction was stopped by incubation for 5 min at to 85 °C; reaction mix was diluted then to a final volume of 400 μl with sterile H_2O.

4.3 siRNA inhibition

For knockdown mRNA expression, cells were reverse-transfected with small inhibitory RNA (siRNA, oligonucletides shown in Table 2) using Lipofectamine RNAiMAX reagent (Invitrogen, Carlsbad, CA, USA). The positive surface charge of the liposome formed by reagent interacts with the siRNA oligonucleotides, allowing them to enter the cell through the negatively charged cell membrane. Three specific double-stranded oligos against a particular gene were used simultaneously and single unspecific control oligonucleotide was used as a control. Control transfection was always performed for same time points as for siRNA-transfection. First, the siRNA oligonucleotides (Eurogentec, 200 pmol of each or 600 pmol of control) were diluted to 500 μl of cell culture medium, but without antibiotics and serum. Then 5 μl RNAiMAX reagent was added and the mixture was incubated for 15-20 min at room temperature and laid to 6-well plates. MCF-10A cells (350,000) were added in 2.5 ml of medium with serum into the wells. The transfection was continued for 24 h before ligand treatment. RNA extraction and cDNA synthesis of treated cells were done as described previously. Transfection efficiency was monitored by measuring mRNA expression of the silenced gene from both control and siRNA samples with RT-qPCR and Western blot analysis.

Table 2. siRNA oligonucleotides. Location (relative to the TSS) and sequence of siRNA oligonucleotides used for gene-specific knockdown.

Target gene	Location	Sequence of + oligonucleotide (5' - 3')
Control	-	UGCGCUACGAUCGACGAUG
HDAC4	1117 1521 3279	CGAGCACAUCAAGCAACAA CAGCUUCUGAACCGAAUCU GCGUGAGCAAGAUCCUCAU
HDAC6	174 1771 2621	GUGUCACUUCGAAGCGAAA CCGUGAGAGUUCCAACUUU GGACCCUCCAGUUCUAAGU

4.4 PCR-primer design

RT-qPCR primers were designed with Oligo 4.0-s-software (National Biosciences, Plymouth, MN, USA). Primers for mRNA quantification (Table 3) were designed in a manner that either another primer overlaps with two exons, or there exists a large (several thousand base pairs) intron between primers to prevent possible replication of genomic DNA contamination in cDNA samples. Other primers were designed to achieve annealing energy of primer itself or between primer pair to be as near to zero as possible. Acceptable dimerization energy was between 0 and -5 kcal/mol. If possible, primers were designed to end with a C or a G at 3' end. PCR-product length was between 80 and 150 bp and no hairpin formation was accepted. Specificity of designed primers was determined with nucleotide-BLAST searches from human genome or transcriptome database maintained by National Center for Biotechnology Information (NCBI). A criterion for specificity was that primer sequence is unique for DNA or cDNA sequence of interest and no exception were accepted. The designed primers were produced by Oligomer (Oligomer, Helsinki, Finland)

The PCR conditions for the designed primers were optimized with RT-qPCR machines (My-IQ-cycler, BioRad, California, USA) using Maxima™ SYBR Green/Fluorescein qPCR Master Mix 2 × (Fermentas, Vilnius, Lithuania). The reaction was performed with 8 µl of cDNA template and 4 pmol of both forward and reverse primers in total volume of 20

µl. The PCR cycling conditions used were 10 min at 95 °C, 45 cycles for 30 s at 95 °C, for 30 s at 56-66 °C and for 30 s at 72 °C, followed by further elongation for 10 min at 72 °C and melting curve analysis. The primer-specific annealing temperature was determined from Ct-values, melting curve and agarose gel electrophoresis results (Table 3).

Table 3. RT-qPCR primers. Sequences, product sizes and annealing temperatures of primer pairs used for gene-specific RT-qPCR.

Gene	Primer pairs (5' - 3')	Product size (bp)	Annealing temperature (°C)
RPLP0	AGATGCAGCAGATCCGCAT GTGGTGATACCTAAAGCCTG	318	58-62
IGFBP3	AAGTTGACTACGAGTCTCAG ACGGCAGGGACCATATTC	83	58
HDAC1	GATCTGCTCCTCTGACAAAC GACTTCTTTCTTCTCCTCTG	159	60
HDAC2	CAGTGGAGATGAAGATGGAG TTTCACCACTGTTGTCCTTG	241	60
HDAC3	CTTCATCCAGATGTCAGCAC TCCACATCGCTTTCCTTGTC	268	60
HDAC4	GCATGTGTTTCTGCCTTGCTG GTTCTCGCAAGTCTGAGCCT	191	60
HDAC5	ATGCTGTTGAAGGACATCTG TCTGGATCTCGATGACTTTC	272	60
HDAC6	GCAAGGGATGGATCTGAACC CTAGGCTGTGAACCAACATC	201	60
HDAC7	CTCACTGTCAGCCCCAGAG TGTCACGCAGGACCACTG	249	62
HDAC8	ACCAGATCTGTGAAAGTGTAC AACTAGACCACATGCTTCAG	414	60
HDAC9	GCAGATCCACATGAACAAACTG GATCTGAGCATCTTCATCACTG	240	60
HDAC10	ATTGAAAGAACAAATGCG CTCTGGGCTCCGTGGGAC	367	62
HDAC11	GGACGACAAGCGTGTGTACATC AGCGGTGTGTCTGAGTTCTGTG	443	60

4.5 RT-qPCR

RT-qPCR was performed with a LightCycler® 480 System (Roche Diagnostic, Mannheim, Germany) using Maxima™ SYBR Green/ Fluorescein qPCR Master Mix 2 × (Fermentas). The reaction was performed with 4 μl of cDNA template and 4 pmol of both forward and reverse primers in a total volume of 10 μl. All primer sequences and primer-specific annealing temperatures are presented in Table 3. In the PCR, DNA was pre-denaturated for 10 min at 95 °C, followed amplification steps cycles (45 cycles) of 20 s denaturation at 95 °C, 20 s annealing at primer-specific temperature and 20 s elongation at 72 °C, followed by further elongation for 10 min at 72 °C and melting curve analysis.

Fold inductions were calculated using the formula $2^{-(\Delta\Delta Ct)}$, where $\Delta\Delta Ct$ is $\Delta Ct_{(stimulus)}$ - $\Delta Ct_{(solvent)}$, ΔCt is $Ct_{(target\ gene)}$ - $Ct_{(contol\ gene)}$. Control gene used was housekeeping gene *ribosomal protein, large, p0 (RPLP0)*. Quality of the PCR product was monitored using post-PCR melt curve analysis. All PCR reactions were done as triplicates and two-tailed Student's t-tests were performed to determinate p-values in reference to non-treated cells to treatments.

4.6 ChIP assay

ChIP was used to determine certain protein binding or histone acetylation level on VDREs on the *IGFBP3* promoter. The cells were seeded into 175 m^2 cell culture bottles with 20 ml medium and grown for 24 h. Before treatments volume of medium was reduced to 10 ml. The cells were stimulated with $1\alpha,25(OH)_2D_3$ or Gemini for indicated time points and nuclear proteins were cross-linked to chromatin by adding formaldehyde directly to the medium to a final concentration of 1%. After 5 min cross-linking at room temperature reaction was stopped by adding glycine (final concentration 0.125 M) and incubating for 5 min at room temperature on rocking platform. Cells were washed twice with ice-cold PBS, scraped into 5 ml PBS and moved to 15 ml tube. To ensure that all cells are transferred to the tube, cell culture bottle was washed twice with 5 ml PBS and washing solution was transferred to the tube. Cells were pelleted by centrifugation (700 × g for 5 min at 4 °C) and the pellet was resuspended in 600 μl of lysis buffer [1% SDS, 10 mM EDTA, 50 mM

Tris-HCl, 1 × protease inhibitor cocktail (Complete, Roche Diagnostic, Mannheim, Germany), pH 8.1] for 10 min at room temperature in 1.5 ml tubes. The lysate was sonicated 10 min by Bioruptor UCD-200 (Diagenode, Liege, Belgium) with intervals of 20 s sonication and 40 s hold in between to result in the majority of DNA fragments being 300-1000 bp in length. Cellular debris was removed by centrifugation for 10-15 min at 4 °C with 16000 × g. For the input samples, 50 µl of the lysate was diluted 1:10 in ChIP dilution buffer (0.01% SDS, 1.1% Triton-X-100, 1.2 mM EDTA, 167 mM NaCl, 16.7 mM Tris-HCl, pH 8.1), stored at 4 °C and further processed as the outputs from step reverse-crosslinking. The remaining lysate was aliquoted to 100 µl aliquots (output samples) and diluted 1:10 in ChIP dilution buffer enriched with 1 × protease inhibitor cocktail and 250 µg/ml of BSA. The output samples were incubated with respective antibodies (Table 4) for overnight at 4 °C on a rocking platform to form immuno-complexes.

The immuno-complexes were collected with 60 µl of protein A agarose slurry (Millipore, Temecula, CA, USA) for 1 h at 4 °C with rotation. EtOH of protein A agarose was changed to ChIP dilution buffer before using it. The beads were pelleted by centrifugation for 1 min at room temperature at 100 × g and washed sequentially 3 min by rotation with 1 ml of the following buffers: low salt wash buffer (0.1% SDS, 1% Triton X-100, 2 mM EDTA, 150 mM NaCl and 20 mM Tris-HCl, pH 8.1), high salt wash buffer (0.1% SDS, 1% Triton X-100, 2 mM EDTA, 500 mM NaCl and 20 mM Tris-HCl, pH 8.1) and LiCl wash buffer (0.25 mM LiCl, 1% Nonidet P-40, 1% sodium deoxycholate, 1 mM EDTA and 10 mM Tris-HCl, pH 8.1). Finally, the beads were washed twice with 1 ml TE buffer (1 mM EDTA and 10 mM Tris-HCl, pH 8.0). After each step beads were pelleted by centrifugation (100 × g for 1 min at room temperature) and the supernatant was aspirated. Immuno-complexes were eluated with 500 µl elution buffer (25 mM Tris-HCl, pH 7.5, 10 mM EDTA, 0.5% SDS) for 30 min at 65 °C.

Remaining proteins were digested from both output and input samples by adding proteinase K (final concentration 80 µg/ml, Fermentas) and simultaneously reverse cross-linked by incubating overnight at 64 °C. The DNA was recovered by phenol/chloroform/isoamyl alcohol (25:24:1, 500 µl per sample) extraction. After centrifugation (14,000 × g for 5 min at room temperature) the supernatant was transferred to fresh tube and DNA was precipitated with 50 µl of 3 M sodium acetate (pH 5.2) and 1

ml of ice-cold EtOH using 1.5 μl glycogen as a carrier (20 mg/ml, Fermentas). The DNA was pelleted with centrifugation (14,000 × g for 20 min at 4 °C) and the pellet was washed with 700 μl ice-cold 70% EtOH. Air-dried input and output samples were dissolved in 100 μl and 50 μl of H_2O, respectively. The difference in final volumes and the difference in the amount of starting material used were taken into account when calculating the PCR results.

Table 4. Antibodies used in chromatin immunoprecipitation.

Antibody target	Code	Amount used	Supplier
IgG	12-370, 1 mg/ml	1 μl per sample	Upstate
VDR	SC-1008, 200 μg/ml	5 μl per sample	Santa Cruz
AcH4	06-866, 1 mg/ml	1 μl per sample	Upstate
HDAC4	SC-11418	5 μl per sample	Santa Cruz
HDAC6	SC-11420	5 μl per sample	Santa Cruz

4.6.1 RT-qPCR of chromatin templates

Two primer pairs were designed to cover two VDREs regions within the *IGFBP3* promoter (Table 5). Quantification of the RT-qPCR products was done using specific TaqMan probes labeled with 6-carboxyfluorescein (FAM) (Eurogentec, Liege, Belgium) (Table 6). The use of these probes ensures that only the particular PCR product of interest is quantified, because unique probe-sequence is complementary to the sequence of PCR product and therefore is targeting only the product of interest.

RT-qPCR was performed with LightCycler® 480 System (Roche Diagnostic, Mannheim, Germany) using Maxima Probe qPCR master mix 2 × (Fermentas, Vilnius, Lithuania). The reaction was performed with 3 μl of ChIP template and 4 pmol of both forward and reverse primers and 0.25 pmol TaqMan probe in a total volume of 10 μl. In the PCR, DNA was

pre-denaturated for 10 min at 95 °C, followed 2-step amplification steps cycles (50 cycles) of 20 s denaturation at 95 °C and 60 s annealing and elongation at 60 °C with all primers.

Relative association of the chromatin bound proteins or histone acetylation level were calculated using the formula [$2^{-(\Delta Cp)}$*100% specific antibody - $2^{-(\Delta Cp)}$*100% non-specific IgG], where ΔCt is the $Ct_{(output)}$-$Ct_{(input)}$ and Ct is the cycle, where the threshold is crossed and normalized by the amount of chromatin used for preparation of input versus output. All PCR reactions were done as triplicates and two-tailed Student's t-tests were performed to determinate P-values in reference to non-treated cells to treatments.

Table 5. ChIP primers. Location (relative to TSS) and sequences of the PCR primer pairs used to detect two genomic regions on *IGFBP3* promoter.

Region	Location	Primer sequence (5' - 3')
RE1/2	- 419 to - 293	CGCTGTATGCCAGTTTCC TCACCCCAGTCACTCCTG
RE3	- 3401 to - 3256	CTCCCACATTGTTTAAGACTC GTAGGCAGTGTGACAGCAG

Table 6. Sequences of FAM-modified qPCR probes. These probes carry at their 5' end a FAM group and were used for the quantification of ChIP products.

Probe target	Location	Primer sequence (5' - 3')
RE1/2	-389 to -369	TCGCCGCAGGGAGACCTCAC
RE3	-3376 to -3351	TCAAATGCCACCACCTCTCAGAAGT

5 RESULTS

5.1 Cyclical induction of *IGFBP3* mRNA expression by 1α,25(OH)$_2$D$_3$

MCF-10A cells were treated with 10 nM 1α,25(OH)$_2$D$_3$ or Gemini in a detailed time course of 240 min with 15 min intervals. RT-qPCR was performed in order to monitor VDR-mediated mRNA induction profile of *IGFBP3* in response to these two VDR ligands. In response to 1α,25(OH)$_2$D$_3$ mRNA induction found to be cyclical and showed peaks after 90, 150 and 210 min, which shows a periodicity of 60 min (Figure 4A). After each peak mRNA level was decreased. In response to Gemini, induction was linear increasing continuously (Figure 4B). Induction of mRNA was also far more stronger in response to Gemini (5.5-fold induction at 240 min) than to 1α,25(OH)$_2$D$_3$ (2.6-fold induction maxima at 210 min). Taken together, in response to 1α,25(OH)$_2$D$_3$ mRNA induction of *IGFBP3* takes place only in 60 min pulses while in response to Gemini mRNA expression is continuously active. The basal level of *IGFBP3* mRNA expression is shown in Figure 12.

5.2 VDR binding to the *IGFBP3* promoter in response to 1α,25(OH)$_2$D$_3$ and Gemini

To study, whether the cyclical changes in *IGFBP3* mRNA expression in response to 1α,25(OH)$_2$D$_3$ is based on VDR binding on the *IGFBP3* promoter, ChIP assay was performed in 1α,25(OH)$_2$D$_3$ and Gemini treated cells with antibody against VDR (Figure 5). ChIP assay was performed over a time period of 150 min. RT-qPCR using TaqMan probes was performed with chromatin templates to determine VDR binding on the two VDREs, RE1/2 and RE3 (Figure 5), located within *IGFBP3* promoter.

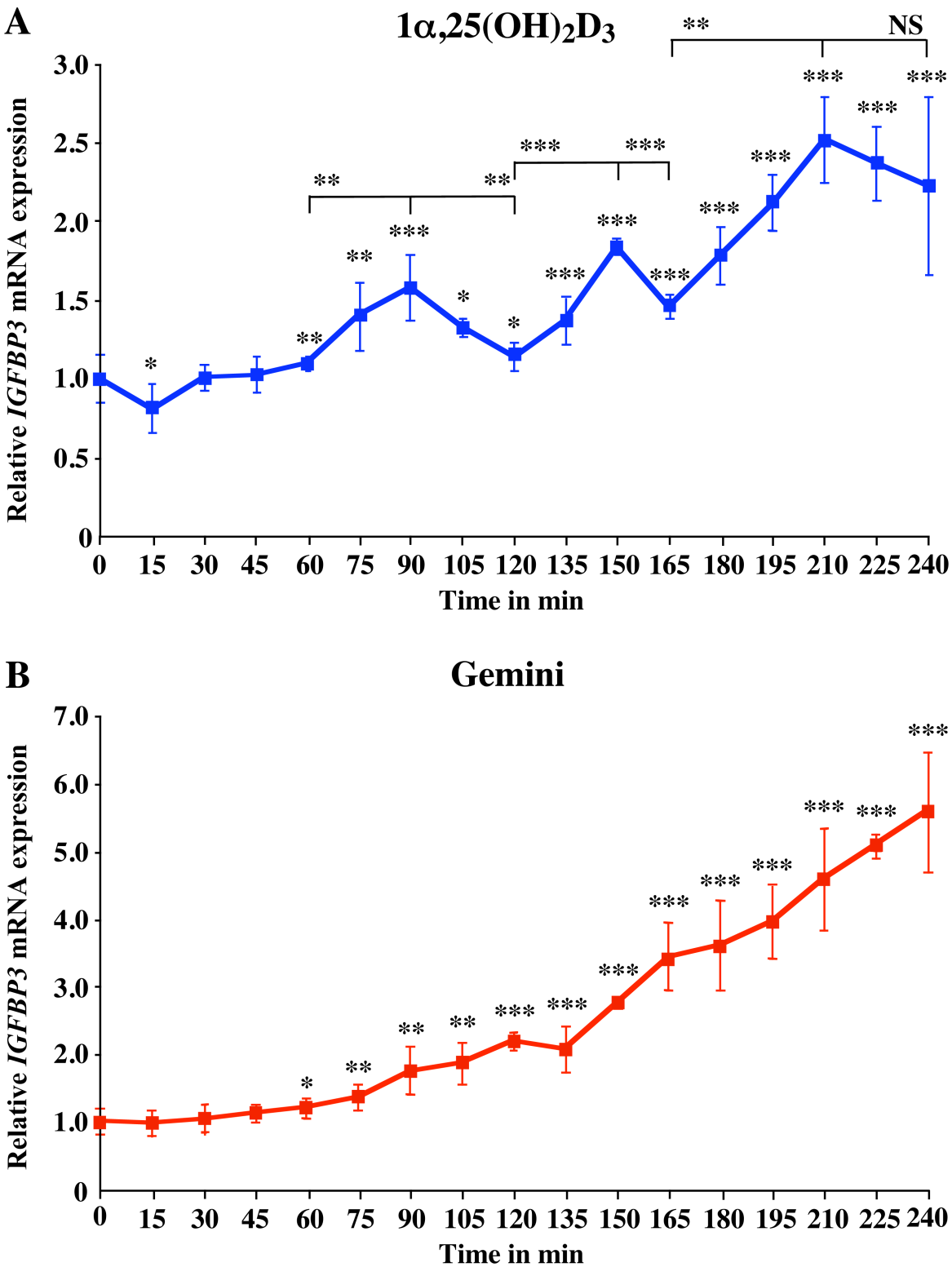

Figure 4. Periodic changes in *IGFBP3* mRNA expression. RT-qPCR was performed to determine the mRNA accumulation of the *IGFBP3* gene in MCF-10A cells after treatment with 10 nM $1\alpha,25(OH)_2D_3$ (A) or Gemini (B) over a time period of 240 min with 15 min intervals. Data points indicate the means of at least three independent experiments and the bars represent standard deviations. A two-tailed Student's t-test was performed to determine the significance of the mRNA induction in reference to solvent control and in comparison of the peaks to the minima (*$p < 0.05$, **$p < 0.01$, ***$p < 0.001$).

In response to 1α,25(OH)$_2$D$_3$ treatment, binding of VDR was cyclical and showed peaks at 30 and 105 min in both VDRE regions (Figure 5A and C). After Gemini treatment VDR did not showed any cyclical association on RE1/2 (Figure 5B). In addition, no significant increase in VDR binding compared to time point 0 was observed. Gemini increased VDR binding on RE3 in cyclical fashion showing maximal levels at 45 and 120 min (Figure 5D).

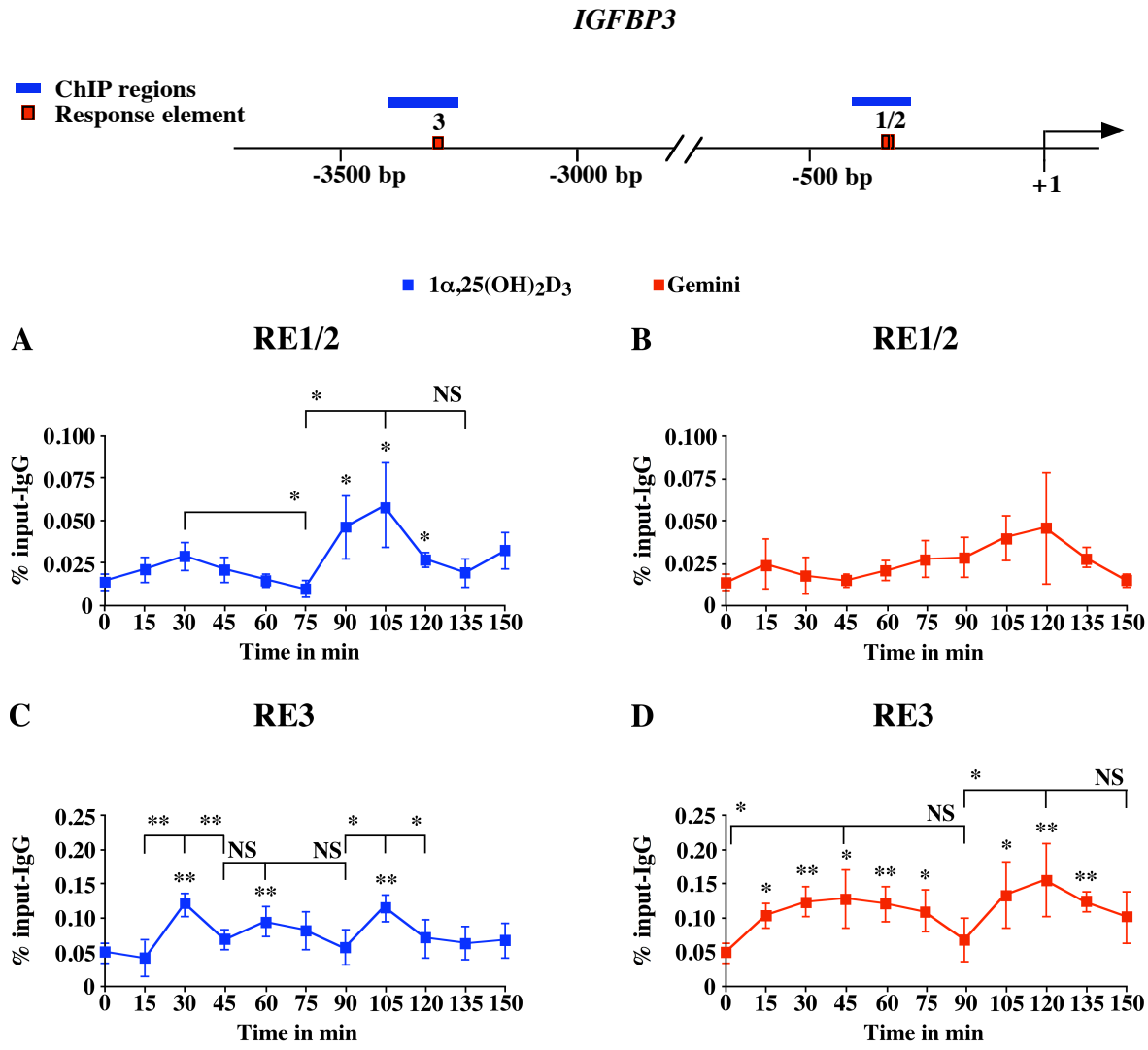

Figure 5. Dynamic association of VDR with RE1/2 (A and B) and RE3 (B and D) on the *IGFBP3* promoter. ChIP assay using anti-VDR antibodies was performed on chromatin extracts from MCF-10A cells treated for indicated time points with 10 nM 1α,25(OH)$_2$D$_3$ (A and C) or Gemini (B and D). Data points indicate the means of at least three independent experiments and the bars represent standard deviations. A two-tailed Student's t-test was performed to determine the significance of the time-dependent association of VDR in reference to time point 0 and in comparison of the peaks to the minima (*p < 0.05, **p < 0.01, ***p < 0.001).

5.3 Chromatin acetylation in response to 1α,25(OH)$_2$D$_3$ and Gemini

To study general chromatin activation of both VDREs within the *IGFBP3* promoter, ChIP assay with antibodies against acetylated histone 4 (AcH4) was performed in MCF-10A cells that were treated for 30, 60, 90, 120 and 150 min with 1α,25(OH)$_2$D$_3$ or Gemini (Figure 6). On RE1/2 acetylation level of histone 4 stayed induced at 60 min in response to 1α,25(OH)$_2$D$_3$ peaking at 90 min (Figure 6A). In contrast, Gemini treatment caused increased, but relatively stable chromatin acetylation compared to that with 1α,25(OH)$_2$D$_3$. With Gemini treatment acetylation level increased already at 30 min and stayed induced over the whole time period of 150 min. Gemini induced relatively high and stable acetylation level on RE3, while 1α,25(OH)$_2$D$_3$-mediated acetylation was also overall high, but at time points 30 min and 150 min significantly lower than Gemini. In general, acetylation levels of histone 4 in both VDREs were much more complex with 1α,25(OH)$_2$D$_3$ than with Gemini.

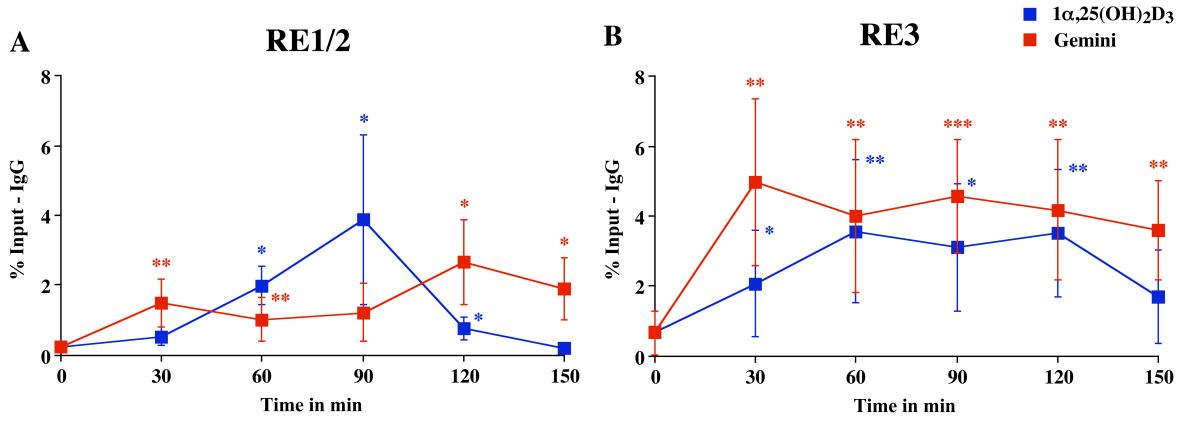

Figure 6. Acetylation level of histone 4 proteins in RE1/2 (A) RE3 (B). ChIP assay using anti-AcH4 antibodies was performed on chromatin extracts from MCF-10A cells treated for indicated time points with 10 nM 1α,25(OH)$_2$D$_3$ or Gemini. Data points indicate the means of at least three independent experiments and the bars represent standard deviations. A two-tailed Student's t-test was performed to determine the significance of the time-dependent acetylation in reference to time point 0 and in comparison of the peaks to the minima (*p < 0.05, **p < 0.01, ***p < 0.001).

5.4 *HDAC*s mRNA expression in response to 1α,25(OH)$_2$D$_3$ and Gemini

Gene expression of every of the 11 *HDAC* genes were studied with RT-qPCR in order to determine if they are primary 1α,25(OH)$_2$D$_3$ or Gemini targets. *HDAC9* was not sufficiently expressed in MCF-10A cell-line to reliably measure with RT-qPCR (Figure 12). Cells, that were treated over a time period of 240 min with 15 min intervals, showed that mRNA expression of only *HDAC4* and *HDAC6* found to be regulated by 1α,25(OH)$_2$D$_3$ (Figure 7A and C), while other *HDAC*s were not significantly regulated by 1α,25(OH)$_2$D$_3$ (Figure 8). In response to 1α,25(OH)$_2$D$_3$ treatment, *HDAC4* was regulated in a cyclical fashion with peaks at 30, 75, 150 and 210 min (Figure 7A), while *HDAC6* showed peaks only at 30 and 75 min. On the contrary, after Gemini treatment was found that neither *HDAC4* nor *HDAC6* was regulated by Gemini (Figure 7B and C). In addition, any of the other *HDAC*s were directly regulated by Gemini (Figure 9).

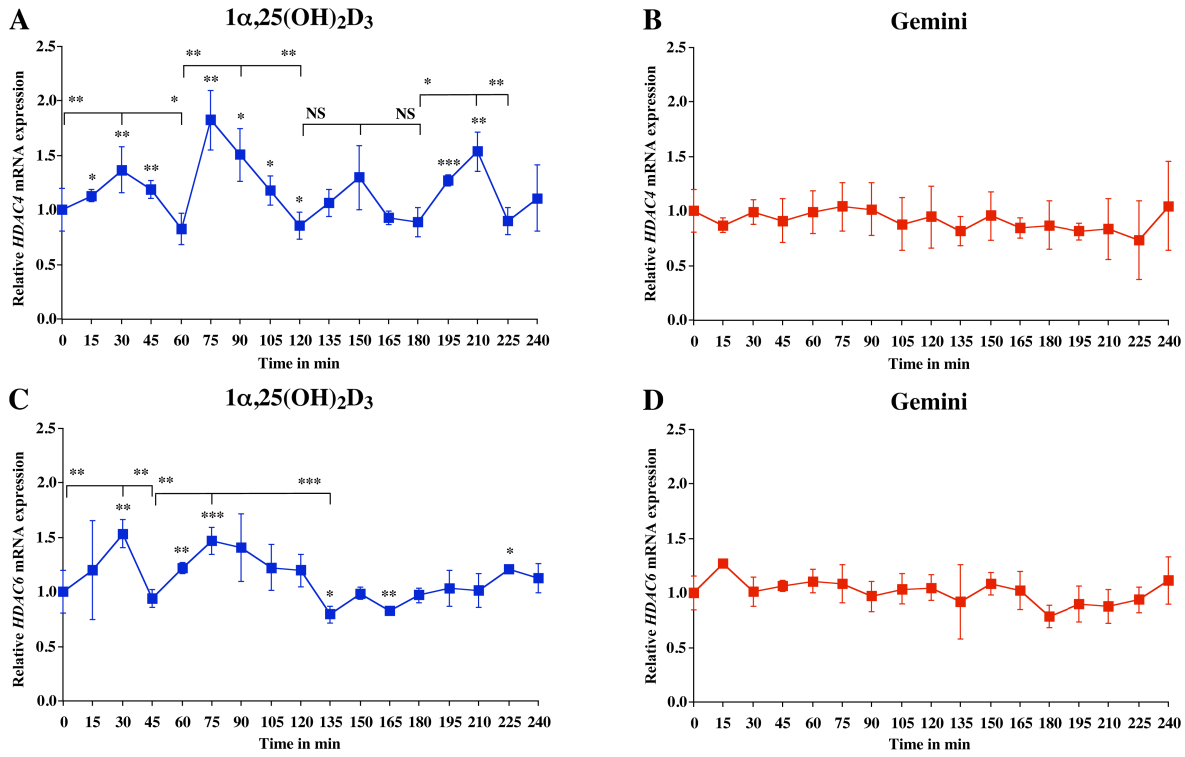

Figure 7. *HDAC4* and *HDAC6* mRNA expression after VDR-ligand treatment. RT-qPCR was performed to determine the mRNA accumulation of the genes *HDAC4* (A and B) and *HDAC6* (C and D) in MCF-10A cells after treatment with 10 nM 1α,25(OH)$_2$D$_3$ (A and C) or Gemini (B and D) over a time period of 240 min with 15 min intervals. Data points indicate the means of at least three independent experiments and the bars represent standard deviations. A two-tailed Student's t-test was performed to determine the significance of the mRNA induction in reference to solvent control and in comparison of the peaks to the minima (*p < 0.05, **p < 0.01, ***p < 0.001).

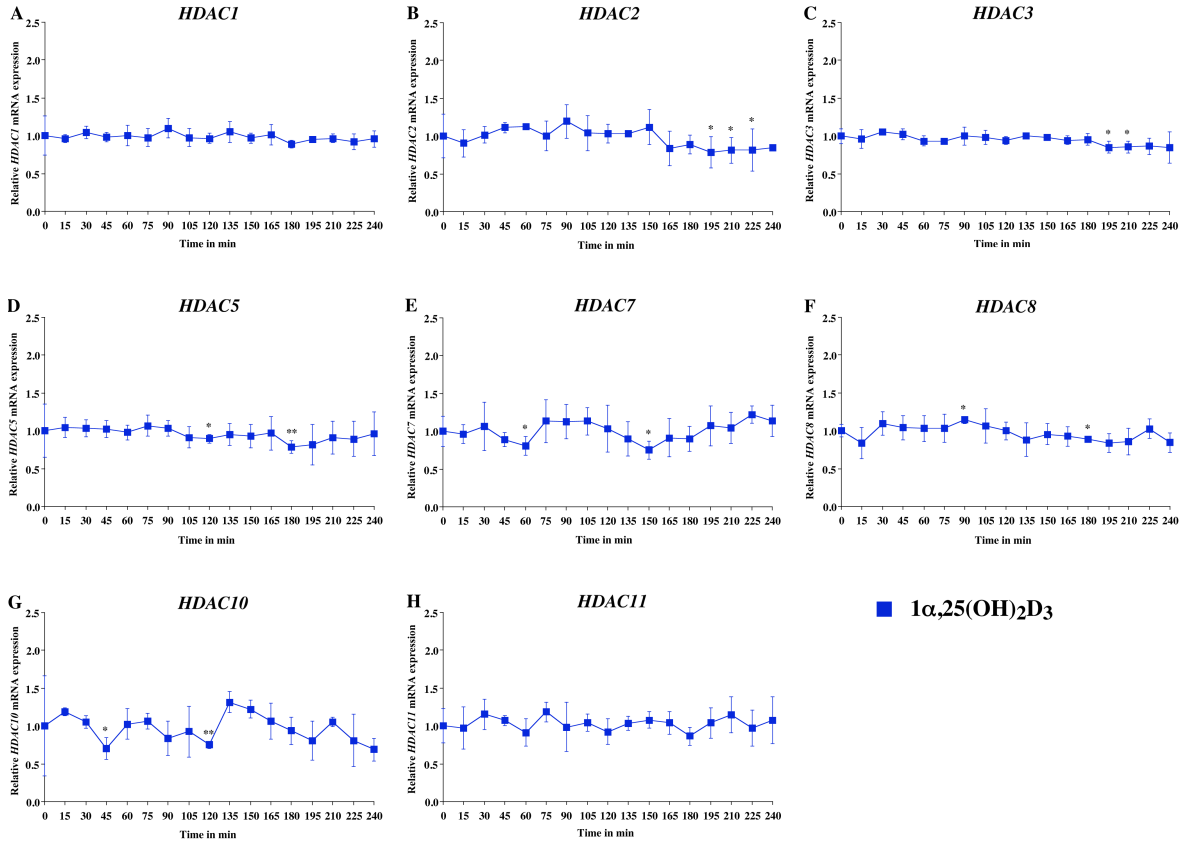

Figure 8. mRNA expression of *HDAC* genes in response to 10 nM 1α,25(OH)$_2$D$_3$. RT-qPCR was performed to determine the mRNA accumulation of the genes *HDAC1, 2, 3, 5, 7, 8, 10* and *11*. in MCF-10A cells after treatment with 10 nM 1α,25(OH)$_2$D$_3$ over a time period of 240 min with 15 min intervals. Data points indicate the means of at least three independent experiments and the bars represent standard deviations. A two-tailed Student's t-test was performed to determine the significance of the mRNA induction in reference to solvent control and in comparison of the peaks to the minima (*p < 0.05, **p < 0.01, ***p < 0.001).

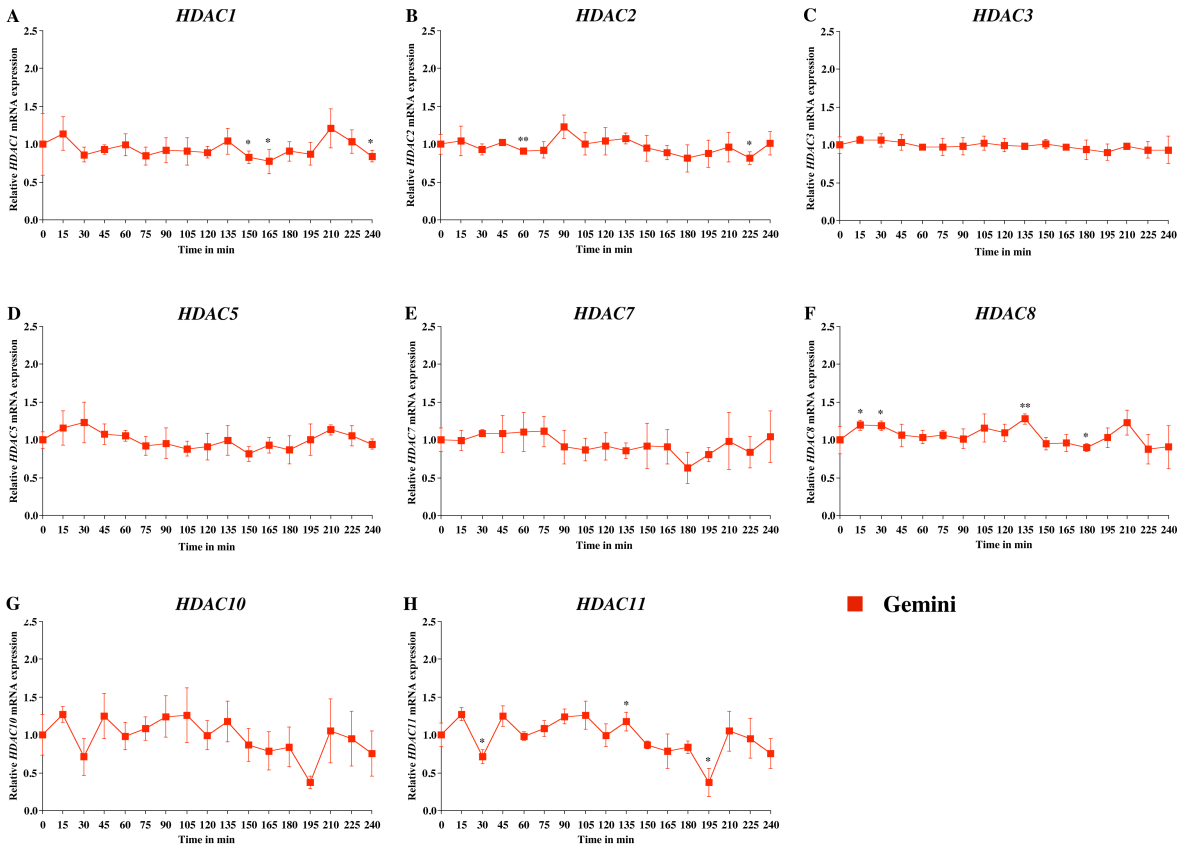

Figure 9. mRNA expression of *HDAC* genes in response to 10 nM Gemini. RT-qPCR was performed to determine the mRNA accumulation of the genes *HDAC1, 2, 3, 5, 7, 8, 10* and *11.* in MCF-10A cells after treatment with 10 nM Gemini over a time period of 240 min with 15 min intervals. Data points indicate the means of at least three independent experiments and the bars represent standard deviations. A two-tailed Student's t-test was performed to determine the significance of the mRNA induction in reference to solvent control and in comparison of the peaks to the minima (*p < 0.05, **p < 0.01, ***p < 0.001).

5.5 Silencing of *HDAC4* and *HDAC6* mRNA expression by siRNA

HDAC4 and *HDAC6* genes were silenced simultaneously in MCF-10A cells by gene-specific siRNA oligonucleotides. 24 h after transfection cells were treated with 1α,25(OH)$_2$D$_3$ over a time period of 120 to 240 min. With control transfection 1α,25(OH)$_2$D$_3$ treatment caused cyclical *IGFBP3* mRNA accumulation showing peaks at 135 and 210 min (Figure 10A). This result corresponds to results from non-transfected cells (Figure 10A). Interestingly, silencing of *HDAC4* and *HDAC6* abolished mRNA cycling of *IGFBP3* caused by 1α,25(OH)$_2$D$_3$ and changes expression to linear (Figure 10C). In contrast, *IGFBP3* mRNA response to Gemini did not change after silencing *HDAC4* and *HDAC6* (Figure 10D) and expression profile was similar to that with control transfection (Figure 10B) or non-transfected cells (Figure 4B).

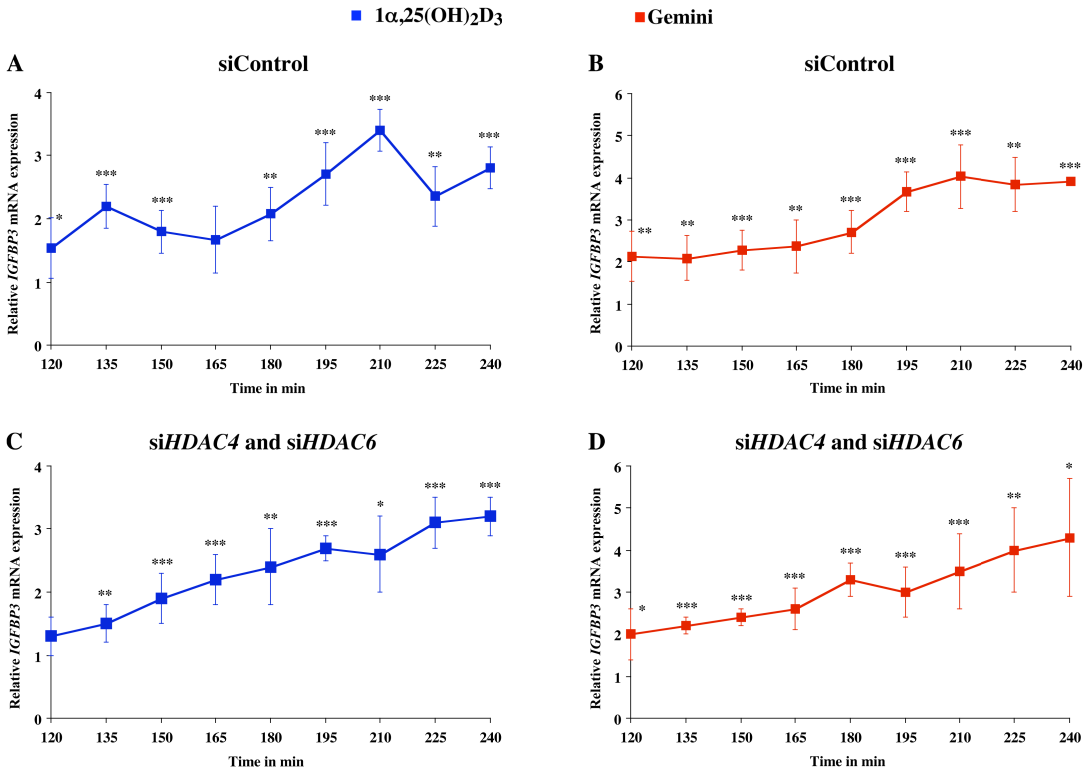

Figure 10. Effect of *HDAC4* and *HDAC6* silencing on the *IGFBP3* mRNA expression. MCF-10A cells were transfected for 24 h with siRNA oligonucleotides against the *HDAC4* and *HDAC6* genes (C and D) or with a non-targeted control siRNA (A and B), and subsequently stimulated for indicated time points with 10 nM 1α,25(OH)$_2$D$_3$ (A and C) or Gemini (B and D). RT-qPCR was performed to determine the mRNA accumulation of *IGFBP3* of indicated siRNA. Data points indicate the means of at least three independent experiments and the bars represent standard deviations. A two-tailed Student's t-test was performed to determine the significance of the mRNA induction in reference to solvent control and in comparison of the peaks to the minima (*$p < 0.05$, **$p < 0.01$, ***$p < 0.001$).

5.6 HDAC4 and HDAC6 association with VDREs on *IGFBP3* promoter

ChIP assay with antibodies against HDAC4 and HDAC6 was performed in cells that were treated over a time period of 150 min with 1α,25$(OH)_2D_3$ or Gemini (Figure 11). At region RE1/2 high basal association with HDAC4 was observed (Figure 11A). In response to 1α,25$(OH)_2D_3$, association found to be cyclical and reduced to minima within 30 min, returned at 60 min and reduced again at 90 min. At region RE3 basal association of HDAC4 was not as strong as at RE3 (Figure 11C). After 1α,25$(OH)_2D_3$ treatment HDAC4 association also reduced to minima at 45 min and slowly increased to normal at 135 min. In response to Gemini, association of HDAC4 reduced within 15 to 45 min on both VDRE regions (Figures 11B and 11D). HDAC4 association was restored at 60 min on both VDREs and stayed high on RE3 and, but decreased again on RE1/2 at time points 120 and 150 min.

In response to 1α,25$(OH)_2D_3$, basal association of HDAC6 reduced at time points 15, 60 and 120 min on RE1/2 (Figure 11E) and at time point 15 min and over a time period of 60 to 120 min on RE3 (Figure 11G). In response to Gemini, HDAC6 association reduced on RE1/2 after 15 min, increased above the basal at 60 and 75 min, reduced to basal at 90 to 120 min, peaked at 135 min and was low at time point 150 min (Figure 11F). After Gemini treatment, HDAC6 association was reduced also on RE3 after 15 min, but stayed low over a time period to 45 min and 105 to 120 min (Figure 11H). In addition, HDAC6 levels were fully restored at time points 60 to 90 min and 135 to 150 min.

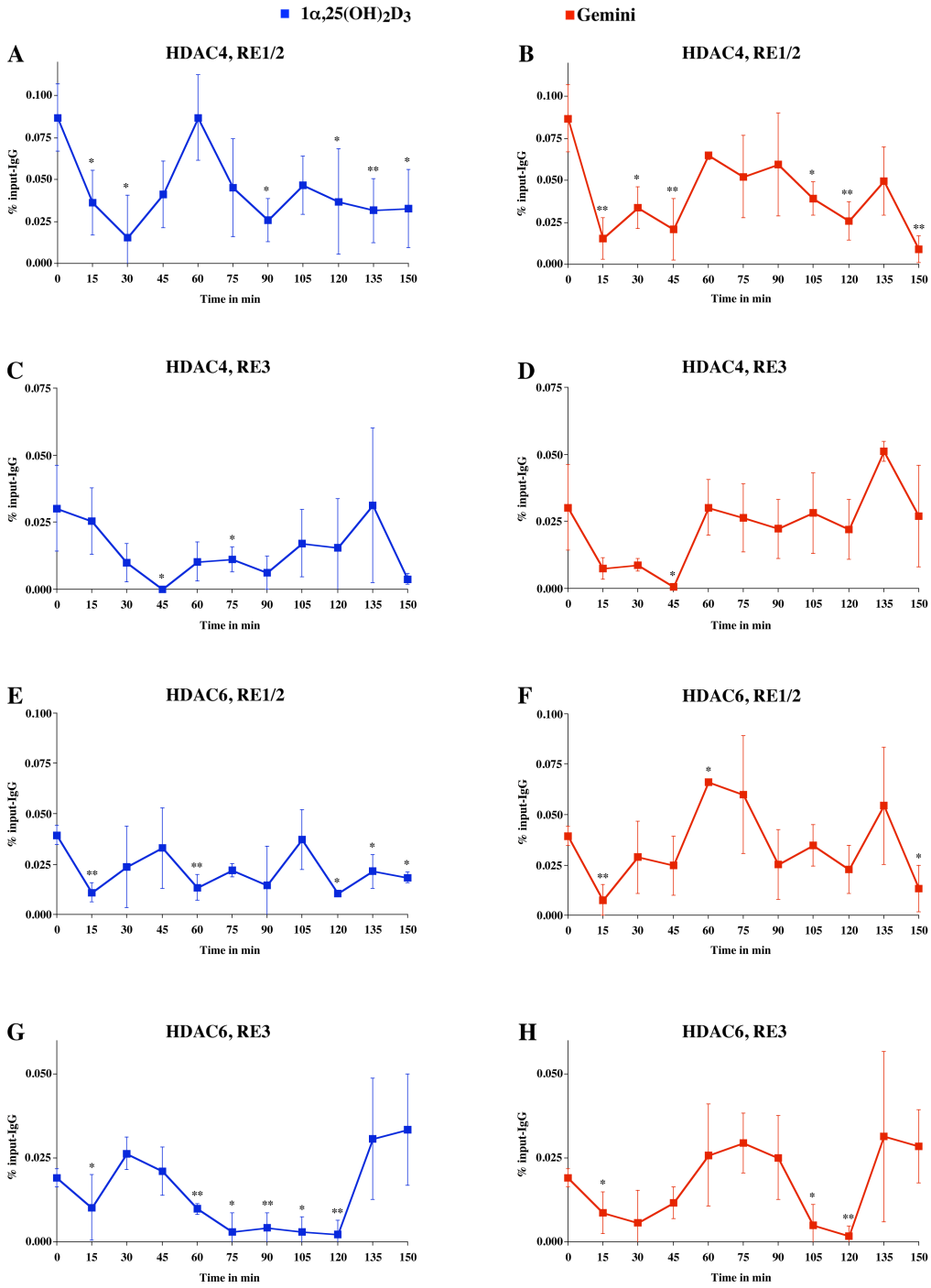

Figure 11. Association of HDAC4 and HDAC6 with RE1/2 and RE3 on the *IGFBP3* promoter. ChIP assay using anti-HDAC4 (A, B, C and D) and anti-HDAC6 (E, F, G and H) antibodies was performed on chromatin extracts from MCF-10A cells treated for indicated time points with 10 nM 1α,25(OH)$_2$D$_3$ (A, C, E and G) or Gemini (B, D, F and H). Data points indicate the means of at least three independent experiments and the bars represent standard deviations. A two-tailed Student's t-test was performed to determine the significance of the time-dependent association of HDAC4 or HDAC6 in reference to time point 0 and in comparison of the peaks to the minima (*$p < 0.05$, **$p < 0.01$, ***$p < 0.001$).

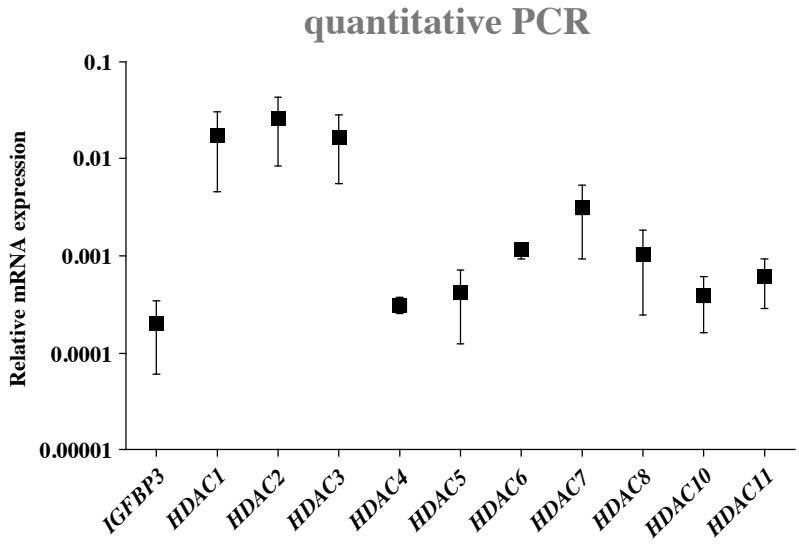

Figure 12. Basal mRNA expression of *HDAC* genes in MCF-10A cells. RT-qPCR was performed to determine the basal mRNA expressions of *IGFBP3* and the 11 *HDAC* genes in relation to the housekeeping gene *RPLP0* in untreated cells. Data points indicate the means of at least three independent experiments and the bars represent standard deviations.

6 DISCUSSION

In this thesis, *IGFBP3* mRNA accumulation was found to be inducible in a different fashion comparing the natural VDR ligand, 1α,25$(OH)_2D_3$, and the synthetic analog Gemini. The *IGFBP3* gene is coding for a well-known growth regulator, is a primary VDR target and of high interest for studying 1α,25$(OH)_2D_3$-mediated growth inhibition in cancer cells. Therefore, it is also a good model for studying the molecular mechanisms of VDR-meditated transcription. In this study, it was found that in response to 1α,25$(OH)_2D_3$, *IGFBP3* mRNA accumulation was cyclical resulting in states of transcriptional activation and repression with a periodicity of 60 min, while the Gemini-induced mRNA accumulation was linear and more stable. Cyclical mRNA expression, mediated by 1α,25$(OH)_2D_3$, led also to reduced total *IGFBP3* induction (2.6-fold), compared to Gemini that showed a 5.5-fold maximal induction at time point 240 min.

Ligand treatment affects gene regulation by activating NR-mediated gene expression. This response is initiated by ligand binding to NRs, which in turn leads to activation of the receptor and subsequently to transcription. However, transcriptional cycling has been reported previously for other NR-activated genes (Métivier *et al.,* 2003; Kim *et al.,* 2005; Degenhardt *et al.,* 2009; Saramäki *et al.,* 2009). Cycling is the result from cyclical association of NRs, their CoAs and CoRs with chromatin. In this study, 1α,25$(OH)_2D_3$ treatment resulted in VDR association in a cyclical fashion with both VDRE regions on the *IGFBP3* promoter. HDAC4 association was also cyclical on RE1/2, but in a different phase than VDR, being lowest when VDR association is peaking. In addition, at RE1/2 chromatin activation corresponds with mRNA accumulation. These results suggest that RE1/2 has probably a more important role in 1α,25$(OH)_2D_3$-mediated *IGFBP3* mRNA cycling than RE3.

Furthermore, histone acetylation levels appeared to be more complex with the natural ligand treatment than with Gemini. In general, histone acetylation is associated with transcriptional activation and deacetylation with transcriptional repression through changes in chromatin condensation (Grunstein, 1997). Therefore, stably increasing chromatin activation observed in both VDRE regions with Gemini treatment correlates with steady mRNA accumulation.

Transcriptional cycling can be divided in to three phases (Degenhardt *et al.,* 2009). Firstly, in the deactivation phase, CoRs and HDACs associate with chromatin keeping it transcriptionally repressed. Secondly, in the activation phase, transcription factors and CoAs replace them. Finally, in the third, initiation phase, VDREs associate with RNA polymerase via mediator proteins resulting in mRNA synthesis. In this study, from the family of HDACs, only HDAC4 and HDAC6 were up-regulated by $1\alpha,25(OH)_2D_3$, but interestingly none of them responded to Gemini. Increased HDAC4 and HDAC6 availability can cause an extended deactivation phase with $1\alpha,25(OH)_2D_3$ treatment. During the transcriptional process, a prolonged deactivation phase results in mRNA degradation, while there is no new mRNA synthesis. This results then in cycling of mRNA accumulation.

Gemini is a synthetic VDR ligand and has a larger volume than $1\alpha,25(OH)_2D_3$, but is still able to fit to the LBP of the VDR (Molnár *et al.,* 2006). In addition, Gemini has been shown to bind more efficiently to LBP than the natural ligand. This leads to prolonged activation phase. Furthermore, Gemini was not able to induce HDAC expression and therefore the cyclical deactivation phase may be shortened. As a result, mRNA synthesis phases are longer and deactivation phases are shorter, which leads to diminished mRNA cycling and more prominent mRNA induction due to more continuous mRNA synthesis.

Interestingly, $1\alpha,25(OH)_2D_3$-mediated transcriptional cycling was abolished when *HDAC4* and *HDAC6* expression was down-regulated by siRNA silencing. This supports the finding that these two HDACs are important components of the $1\alpha,25(OH)_2D_3$-induced transcriptional cycling. However, siRNA silencing does not change the total mRNA induction after 240 min ligand treatment and mRNA levels induced by both ligands remained at the levels of control transfections. This suggests that HDAC4 and HDAC6 are not the only mediators for diverse actions of these ligands, but stronger nature of VDR activation is still observed with Gemini. It should be noted that these ligands are physically different, and they also change conformation of VDR in a different fashion (Molnár *et al.,* 2006). Therefore these findings suggest that HDAC4 and HDAC6 are mediators of transcriptional cycling, but are not the only reason for the diverse nature of these ligands.

However, HDAC4 and HDAC6 association into VDREs were not always congruent with observations of VDR recruitment and histone acetylation. In addition, HDAC6 association

with RE1/2 seemed to be more complex in response to Gemini, than in response to 1α,25(OH)$_2$D$_3$. Due to high standard deviations the interpretation of these results is unclear. And the respective assay will be repeated.

In conclusion, 1α,25(OH)$_2$D$_3$-mediated up-regulation of the *IGFBP3* gene is an interactive process, where cyclical association of VDR, HDAC4, and HDAC6 with VDREs at the *IGFBP3* promoter results in controlled and cyclical induction of mRNA expression. On the other hand, Gemini has far more potent and direct effect on the up-regulation of *IGFBP3* without the cyclical control of transcription. The simplified model illustrates the diverse actions of 1α,25(OH)$_2$D$_3$- and Gemini-induced transcription via the VDR;

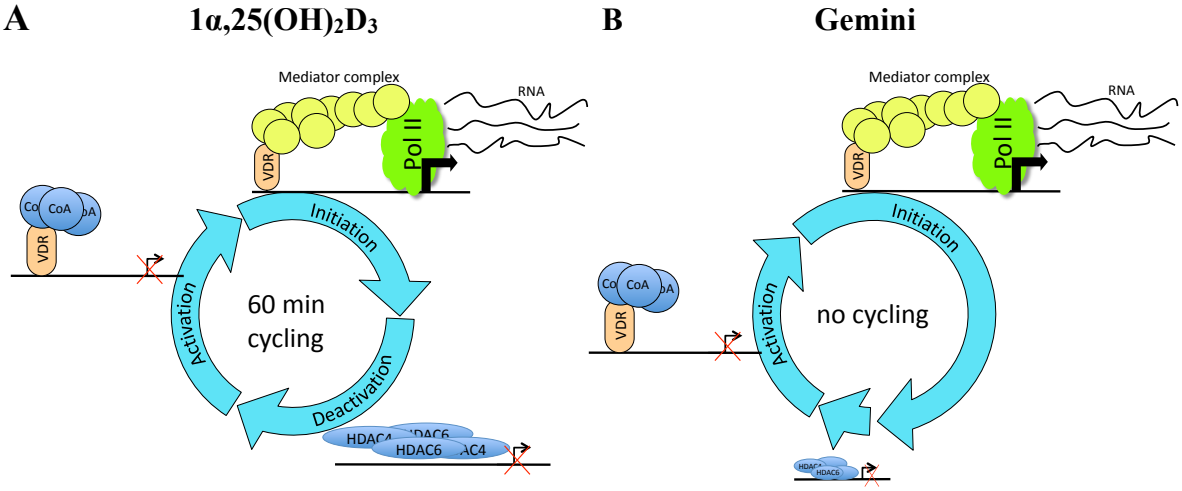

Figure 13. Model for mRNA periodicity in response to 1α,25(OH)$_2$D$_3$ and Gemini. In response to 1α,25(OH)$_2$D$_3$ (A) transcription is divided in three phases, which results in cycling of mRNA accumulation. In response to Gemini (B), the initiation phase is longer due to reduced deactivation phase. This results in more continuous mRNA accumulation.

7 REFERENCES

Andjelkovic, Z., Vojinovic, J., Pejnovic, N., Popovic, M., Dujic, A., Mitrovic, D., Pavlica, L. & Stefanovic, D. (1999). Disease modifying and immunomodulatory effects of high dose 1α(OH)D_3 in rheumatoid arthritis patients. *Clinical and Experimental Rheumatology, 17*(4), 453-456.

Baxter, R. C. (1994). Insulin-like growth factor binding proteins in the human circulation: A review. *Hormone Research, 42*(4-5), 140-144.

Becker, P. B. (2002). Nucleosome sliding: Facts and fiction. *The EMBO Journal, 21*(18), 4749-4753.

Benoit, G., Cooney, A., Giguere, V., Ingraham, H., Lazar, M., Muscat, G., Perlmann, T., Renaud, J., Schwabe, J., Sladek, F., Tsai, M. & Laudet, V. (2006). International union of pharmacology. LXVI. orphan nuclear receptors. *Pharmacological Reviews, 58*(4), 798-836.

Bouillon, R., Verstuyf, A., Verlinden, L., Allewaert, K., Branisteanu, D., Mathieu, C. & van Baelen, H. (1995). Non-hypercalcemic pharmacological aspects of vitamin D analogs. *Biochemical Pharmacology, 50*(5), 577-583.

Bouillon, R., Verstuyf, A., Zhao, J., Tan, B. K. & Van Baelen, H. (1996). Nonhypercalcemic vitamin D analogs: Interactions with the vitamin D-binding protein. *Hormone Research, 45*(3-5), 117-121.

Boyle, B. J., Zhao, X. Y., Cohen, P. & Feldman, D. (2001). Insulin-like growth factor binding protein-3 mediates 1α,25-dihydroxyvitamin D_3 growth inhibition in the LNCaP prostate cancer cell line through p21/WAF1. *The Journal of Urology, 165*(4), 1319-1324.

Brownell, J. E. & Allis, C. D. (1996). Special HATs for special occasions: Linking histone acetylation to chromatin assembly and gene activation. *Current Opinion in Genetics & Development, 6*(2), 176-184.

Buckbinder, L., Talbott, R., Velasco-Miguel, S., Takenaka, I., Faha, B., Seizinger, B. R. & Kley, N. (1995). Induction of the growth inhibitor IGF-binding protein 3 by p53. *Nature, 377*(6550), 646-649.

Bury, Y., Ruf, D., Hansen, C. M., Kissmeyer, A. M., Binderup, L. & Carlberg, C. (2001). Molecular evaluation of vitamin D_3 receptor agonists designed for topical treatment of skin diseases. *The Journal of Investigative Dermatology, 116*(5), 785-792.

Butt, A. J., Fraley, K. A., Firth, S. M. & Baxter, R. C. (2002). IGF-binding protein-3-induced growth inhibition and apoptosis do not require cell surface binding and nuclear translocation in human breast cancer cells. *Endocrinology, 143*(7), 2693-2699.

Carlberg, C. (2004). Ligand-mediated conformational changes of the VDR are required for gene transactivation. *The Journal of Steroid Biochemistry and Molecular Biology, 89-90*(1-5), 227-232.

Carlberg, C. & Molnár, F. (2006). Detailed molecular understanding of agonistic and antagonistic vitamin D receptor ligands. *Current Topics in Medicinal Chemistry, 6*(12), 1243-1253.

Carlberg, C. & Mourino, A. (2003). New vitamin D receptor ligands. *Expert opinion on therapeutic patents, 13*(6), 761-772.

Carlberg, C. & Polly, P. (1998). Gene regulation by vitamin D_3. *Critical Reviews in Eukaryotic Gene Expression, 8*(1), 19-42.

Carlberg, C., Dunlop, T. W., Saramäki, A., Sinkkonen, L., Matilainen, M. & Väisänen, S. (2007). Controlling the chromatin organization of vitamin D target genes by multiple vitamin D receptor binding sites. *The Journal of Steroid Biochemistry and Molecular Biology, 103*(3-5), 338-343.

Castillo, A., Jimenez-Lara, A., Tolon, R. & Aranda, A. (1999). Synergistic activation of the prolactin promoter by vitamin D receptor and GHF-1: Role of the coactivators, CREB-binding protein and steroid hormone receptor coactivator-1 (SRC-1). *Molecular Endocrinology, 13*(7), 1141-1154.

Chawla, A., Repa, J. J., Evans, R. M. & Mangelsdorf, D. J. (2001). Nuclear receptors and lipid physiology: Opening the X-files. *Science (Washington), 294*(5548), 1866-1870.

Colston, K. W., Perks, C. M., Xie, S. P. & Holly, J. M. (1998). Growth inhibition of both MCF-7 and Hs578T human breast cancer cell lines by vitamin D analogues is associated with increased expression of insulin-like growth factor binding protein-3. *Journal of Molecular Endocrinology, 20*(1), 157-162.

de Ruijter, A. J. M., van Gennip, A. H., Caron, H. N., Kemp, S. & van Kuilenburg, A. B. P. (2003). Histone deacetylases (HDACs): Characterization of the classical HDAC family. *The Biochemical Journal, 370*(3), 737-749.

Deeb, K. K., Trump, D. L. & Johnson, C. S. (2007). Vitamin D signalling pathways in cancer: Potential for anticancer therapeutics. *Nature Reviews: Cancer, 7*(9), 684-700. doi:10.1038/nrc2196

Degenhardt, T., Rybakova, K., Tomaszewska, A., Mone, M., Westerhoff, H., Bruggeman, F. & Carlberg, C. (2009). Population-level transcription cycles derive from stochastic timing of single-cell transcription. *Cell, 138*(3), 489-501.

DeLuca, H. F. (2004). Overview of general physiologic features and functions of vitamin D. *The American Journal of Clinical Nutrition, 80*(6 Suppl), 1689S-96S.

Elgin, S. C. R. & Grewal, S. I. S. (2003). Heterochromatin: Silence is golden. *Current Biology : CB, 13*(23), R895-8.

Felsenfeld, G. & Groudine, M. (2003). Controlling the double helix. *Nature, 421*(6921), 448-453.

Fischle, W., Dequiedt, F., Fillion, M., Hendzel, M., Voelter, W. & Verdin, E. (2001). Human HDAC7 histone deacetylase activity is associated with HDAC3 in vivo. *Journal of Biological Chemistry, 276*(38), 35826-35835.

Fischle, W., Dequiedt, F., Hendzel, M., Guenther, M., Lazar, M., Voelter, W. & Verdin, E. (2002). Enzymatic activity associated with class II HDACs is dependent on a multiprotein complex containing HDAC3 and SMRT/N-CoR. *Molecular Cell, 9*(1), 45-57.

Garland, C., Garland, F., Gorham, E., Lipkin, M., Holick, M. & et al. (2006). The role of vitamin D in cancer prevention. *American Journal of Public Health, 96*(2), 252-261.

Gilbert, N., Boyle, S., Fiegler, H., Woodfine, K., Carter, N. & Bickmore, W. (2004). Chromatin architecture of the human genome gene-rich domains are enriched in open chromatin fibers. *Cell, 118*(5), 555-566.

Gill, G. (2004). SUMO and ubiquitin in the nucleus: Different functions, similar mechanisms? *Genes & Development, 18*(17), 2046-2059.

Gonzalez, M. M., Samenfeld, P., Peräkylä, M. & Carlberg, C. (2003). Corepressor excess shifts the two-side chain vitamin D analog gemini from an agonist to an inverse agonist of the vitamin D receptor. *Molecular Endocrinology (Baltimore, Md.), 17*(10), 2028-2038.

Gregoretti, I., Lee, Y. & Goodson, H. (2004). Molecular evolution of the histone deacetylase family: Functional implications of phylogenetic analysis. *Journal of Molecular Biology, 338*(1), 17-31.

Gregori, S., Giarratana, N., Smiroldo, S., Uskokovic, M. & Adorini, L. (2002). A 1α,25-dihydroxyvitamin D_3 analog enhances regulatory T-cells and arrests autoimmune diabetes in NOD mice. *Diabetes, 51*(5), 1367-1374.

Grunstein, M. (1997). Histone acetylation in chromatin structure and transcription. *Nature, 389*(6649), 349-352.

Guler, H. P., Zapf, J., Schmid, C. & Froesch, E. R. (1989). Insulin-like growth factors I and II in healthy man. estimations of half-lives and production rates. *Acta Endocrinologica, 121*(6), 753-758.

Hansen, J. (2002). Conformational dynamics of the chromatin fiber in solution: Determinants, mechanisms, and functions. *Annual Review of Biophysics and Biomolecular Structure, 31*, 361-392.

Haussler, M., Whitfield, G., Haussler, C., Hsieh, J., Thompson, P., Selznick, S., Dominguez, C. & Jurutka, P. (1998). The nuclear vitamin D receptor: Biological and molecular regulatory properties revealed. *Journal of Bone and Mineral Research, 13*(3), 325-349.

Herdick, M., Bury, Y., Quack, M., Uskokovic, M. R., Polly, P. & Carlberg, C. (2000). Response element and coactivator-mediated conformational change of the vitamin D_3 receptor permits sensitive interaction with agonists. *Molecular Pharmacology, 57*(6), 1206-1217.

Hollis, B. W. (2005). Circulating 25-hydroxyvitamin D levels indicative of vitamin D sufficiency: Implications for establishing a new effective dietary intake recommendation for vitamin D. *Journal of Nutrition, 135*(2), 317-322.

Horn, P. & Peterson, C. (2002). Chromatin higher order folding: Wrapping up transcription. *Science (Washington), 297*(5588), 1824-1827.

Hwa, V., Oh, Y. & Rosenfeld, R. G. (1999). The insulin-like growth factor-binding protein (IGFBP) superfamily. *Endocrine Reviews, 20*(6), 761-787.

Hyppönen, E., Läärä, E., Reunanen, A., Järvelin, M. R. & Virtanen, S. M. (2001). Intake of vitamin D and risk of type 1 diabetes: A birth-cohort study. *Lancet, 358*(9292), 1500-1503.

Ingraham, B. A., Bragdon, B. & Nohe, A. (2008). Molecular basis of the potential of vitamin D to prevent cancer. *Current Medical Research and Opinion, 24*(1), 139-149.

Jaques, G., Noll, K., Wegmann, B., Witten, S., Kogan, E., Radulescu, R. T. & Havemann, K. (1997). Nuclear localization of insulin-like growth factor binding protein 3 in a lung cancer cell line. *Endocrinology, 138*(4), 1767-1770.

Jenuwein, T. & Allis, C. D. (2001). Translating the histone code. *Science, 293*(5532), 1074-1080.

Karas, M., Danilenko, M., Fishman, D., LeRoith, D., Levy, J. & Sharoni, Y. (1997). Membrane-associated insulin-like growth factor-binding protein-3 inhibits insulin-like growth factor-I-induced insulin-like growth factor-I receptor signaling in ishikawa endometrial cancer cells. *Journal of Biological Chemistry, 272*(26), 16514-16520.

Kim, S., Shevde, N. K. & Pike, J. W. (2005). 1,25-dihydroxyvitamin D_3 stimulates cyclic vitamin D receptor/retinoid X receptor DNA-binding, co-activator recruitment, and histone acetylation in intact osteoblasts. *Journal of Bone and Mineral Research : The Official Journal of the American Society for Bone and Mineral Research, 20*(2), 305-317.

Leal, S., Liu, Q., Huang, S. S. & Huang, J. S. (1997). The type V transforming growth factor beta receptor is the putative insulin-like growth factor-binding protein 3 receptor. *Journal of Biological Chemistry, 272*(33), 20572-20576.

Lee, K., Ma, L., Yan, X., Liu, B., Zhang, X. & Cohen, P. (2005). Rapid apoptosis induction by IGFBP-3 involves an insulin-like growth factor-independent nucleomitochondrial translocation of RXRα/Nur77. *Journal of Biological Chemistry, 280*(17), 16942-16948.

Leo, C. & Chen J. D. (2000). The SRC family of nuclear receptor coactivators. *Gene, 245*(1), 1-11.

Li, Y., Lambert, M. & Xu, H. (2003). Activation of nuclear receptors A perspective from structural genomics. *Structure, 11*(7), 741-746.

Li, Y. M., Schacher, D. H., Liu, Q., Arkins, S., Rebeiz, N., McCusker, R. H.,Jr, Dantzer, R. & Kelley, K. W. (1997). Regulation of myeloid growth and differentiation by the insulin-like growth factor I receptor. *Endocrinology, 138*(1), 362-368.

Lips, P. (2006). Vitamin D physiology. *Progress in Biophysics and Molecular Biology, 92*(1), 4-8.

Liu, B., Lee, H., Weinzimer, S., Powell, D., Clifford, J., Kurie, J. & Cohen, P. (2000). Direct functional interactions between insulin-like growth factor-binding protein-3 and retinoid X receptor- α regulate transcriptional signaling and apoptosis. *Journal of Biological Chemistry, 275*(43), 33607-33613.

Luger, K., Mader, A., Richmond, R., Sargent, D. & Richmond, T. (1997). Crystal structure of the nucleosome core particle of chromatin at 2.8 ångström resolution. Boston, MA (USA).

Mathiasen, I. S., Lademann, U. & Jäättelä, M. (1999). Apoptosis induced by vitamin D compounds in breast cancer cells is inhibited by bcl-2 but does not involve known caspases or p53. *Cancer Research, 59*(19), 4848-4856.

Mathieu, C., Waer, M., Casteels, K., Laureys, J. & Bouillon, R. (1995). Prevention of type I diabetes in NOD mice by nonhypercalcemic doses of a new structural analog of 1,25-dihydroxyvitamin D3, KH1060. *Endocrinology, 136*(3), 866-872.

Mathieu, C., Waer, M., Laureys, J., Rutgeerts, O. & Bouillon, R. (1994). Prevention of autoimmune diabetes in NOD mice by 1,25 dihydroxyvitamin D3. *Diabetologia, 37*(6), 552-558.

Matilainen, M., Malinen, M., Saavalainen, K. & Carlberg, C. (2005). Regulation of multiple insulin-like growth factor binding protein genes by 1α,25-dihydroxyvitamin D_3. *Nucleic Acids Research, 33*(17), 5521-5532.

Mattner, F., Smiroldo, S., Galbiati, F., Muller, M., Di Lucia, P., Poliani, P., Martino, G., Panina-Bordignon, P. & Adorini, L. (2000). Inhibition of Th1 development and treatment of chronic-relapsing experimental allergic encephalomyelitis by a non-hypercalcemic analogue of 1,25-dihydroxyvitamin D_3. *European Journal of Immunology, 30*(2), 498-508.

McKenna, N. & O'Malley, B. (2002). Combinatorial control of gene expression by nuclear receptors and coregulators. *Cell, 108*(4), 465-474.

Métivier, R., Penot, G., Hübner, M. R., Reid, G., Brand, H., Kos, M. & Gannon, F. (2003). Estrogen receptor-α directs ordered, cyclical, and combinatorial recruitment of cofactors on a natural target promoter. *Cell, 115*(6), 751-763.

Molnár, F., Peräkylä, M. & Carlberg, C. (2006). Vitamin D receptor agonists specifically modulate the volume of the ligand-binding pocket. *Journal of Biological Chemistry, 281*(15), 10516-10526.

Munger, K. L., Levin, L. I., Hollis, B. W., Howard, N. S. & Ascherio, A. (2006). Serum 25-hydroxyvitamin D levels and risk of multiple sclerosis. *JAMA: Journal of the American Medical Association, 296*(23), 2832-2838.

Nagpal, S., Na, S. & Rathnachalam, R. (2005). Noncalcemic actions of vitamin D receptor ligands. *Endocrine Reviews, 26*(5), 662-687.

Nickerson, T. & Huynh, H. (1999). Vitamin D analogue EB1089-induced prostate regression is associated with increased gene expression of insulin-like growth factor binding proteins. *The Journal of Endocrinology, 160*(2), 223-229.

Norman, A. W., Manchand, P. S., Uskokovic, M. R., Okamura, W. H., Takeuchi, J. A., Bishop, J. E., Hisatake, J. I., Koeffler, H. P. & Peleg, S. (2000). Characterization of a novel analogue of 1α,25$(OH)_2$-vitamin D_3 with two side chains: Interaction with its nuclear receptor and cellular actions. *Journal of Medicinal Chemistry, 43*(14), 2719-2730.

Peng, L., Malloy, P. J. & Feldman, D. (2004). Identification of a functional vitamin D response element in the human insulin-like growth factor binding protein-3 promoter. *Molecular Endocrinology (Baltimore, Md.), 18*(5), 1109-1119.

Polly, P., Herdick, M., Moehren, U., Baniahmad, A., Heinzel, T. & Carlberg, C. (2000). VDR-alien: A novel, DNA-selective vitamin D_3 receptor-corepressor partnership. *The FASEB Journal : Official Publication of the Federation of American Societies for Experimental Biology, 14*(10), 1455-1463.

Quack, M. & Carlberg, C. (2000). Ligand-triggered stabilization of vitamin D Receptor/Retinoid X receptor heterodimer conformations on DR4-type response elements. *Journal of Molecular Biology, 296*(3), 743-756.

Rachez, C., Lemon, B., Suldan, Z., Bromleigh, V., Gamble, M., Naeaer, A., Erdjument-Bromage, H., Tempst, P. & Freedman, L. (1999). Ligand-dependent transcription activation by nuclear receptors requires the DRIP complex. *Nature, 398*(6730), 824-828.

Rachez, C., Suldan, Z., Ward, J., Chang, C. P., Burakov, D., Erdjument-Bromage, H., Tempst, P. & Freedman, L. P. (1998). A novel protein complex that interacts with the vitamin D_3 receptor in a ligand-dependent manner and enhances VDR transactivation in a cell-free system. *Genes & Development, 12*(12), 1787-1800.

Renehan, A. G., Harvie, M. & Howell, A. (2006). Insulin-like growth factor (IGF)-I, IGF binding protein-3, and breast cancer risk: Eight years on. *Endocrine-Related Cancer, 13*(2), 273-278.

Saramäki, A., Diermeier, S., Kellner, R., Laitinen, H., Väisanen, S. & Carlberg, C. (2009). Cyclical chromatin looping and transcription factor association on the regulatory regions of the p21 (CDKN1A) gene in response to 1α,25-dihydroxyvitamin D_3. *Journal of Biological Chemistry, 284*(12), 8073-8082.

Schedlich, L. J., Young, T. F., Firth, S. M. & Baxter, R. C. (1998). Insulin-like growth factor-binding protein (IGFBP)-3 and IGFBP-5 share a common nuclear transport pathway in T47D human breast carcinoma cells. *The Journal of Biological Chemistry, 273*(29), 18347-18352.

Schräder, M., Nayeri, S., Kahlen, J. P., Müller, K. M. & Carlberg, C. (1995). Natural vitamin D_3 response elements formed by inverted palindromes: Polarity-directed ligand sensitivity of vitamin D_3 receptor-retinoid X receptor heterodimer-mediated transactivation. *Molecular and Cellular Biology, 15*(3), 1154-1161.

Spotswood, H. T. & Turner, B. M. (2002). An increasingly complex code. *The Journal of Clinical Investigation, 110*(5), 577-582.

Suda, T., Ueno, Y., Fujii, K. & Shinki, T. (2003). Vitamin D and bone. *Journal of Cellular Biochemistry, 88*(2), 259-266.

Toell, A., Polly, P. & Carlberg, C. (2000). All natural DR3-type vitamin D response elements show a similar functionality in vitro. *The Biochemical Journal, 352 Pt 2*, 301-309.

Turner, B. (2002). Cellular memory and the histone code. *Cell, 111*(3), 285-291.

Umesono, K., Murakami, K. K., Thompson, C. C. & Evans, R. M. (1991). Direct repeats as selective response elements for the thyroid hormone, retinoic acid, and vitamin D3 receptors. *Cell, 65*(7), 1255-1266.

Veldman, C. M., Cantorna, M. T. & DeLuca, H. F. (2000). Expression of 1,25-dihydroxyvitamin D_3 receptor in the immune system. *Archives of Biochemistry and Biophysics, 374*(2), 334-338.

Väisänen, S., Peräkylä, M., Kärkkäinen, J. I., Uskokovic, M. R. & Carlberg, C. (2003). Structural evaluation of the agonistic action of a vitamin D analog with two side chains binding to the nuclear vitamin D_3 receptor. *Molecular Pharmacology, 63*(6), 1230-1237.

van den Bemd, G. C., Pols, H. A., Birkenhager, J. C. & van Leeuwen, J. P. (1996). Conformational change and enhanced stabilization of the vitamin D receptor by the 1,25-dihydroxyvitamin D_3 analog KH1060. *Proceedings of the National Academy of Sciences of the United States of America, 93*(20), 10685-10690.

Varga-Weisz, P. D., Blank, T. A. & Becker, P. B. (1995). Energy-dependent chromatin accessibility and nucleosome mobility in a cell-free system. *The EMBO Journal, 14*(10), 2209-2216.

Verdin, E., Dequiedt, F. & Kasler, H. (2003). Class II histone deacetylases: Versatile regulators. *Trends in Genetics, 19*(5), 286-293.

Verlinden, L., Verstuyf, A., Convents, R., Marcelis, S., Van Camp, M. & Bouillon, R. (1998). Action of 1,25(OH)$2D_3$ on the cell cycle genes, cyclin D1, p21 and p27 in MCF-7 cells. *Molecular and Cellular Endocrinology, 142*(1-2), 57-65.

Wasserman, R. H. & Fullmer, C. S. (1995). Vitamin D and intestinal calcium transport: Facts, speculations and hypotheses. *The Journal of Nutrition, 125*(7 Suppl), 1971S-1979S.

Wegel, E. & Shaw, P. (2005). Gene activation and deactivation related changes in the three-dimensional structure of chromatin. *Chromosoma, 114*(5), 331-337.

Welsh, J. (2007) a. Vitamin D and prevention of breast cancer. *Acta Pharmacologica Sinica, 28*(9), 1373-1382.

Welsh, J. (2007) b. Targets of vitamin D receptor signaling in the mammary gland. *Journal of Bone and Mineral Research, 22*(12; Suppl.), V86-90.

Xie, S. P., Pirianov, G. & Colston, K. W. (1999). Vitamin D analogues suppress IGF-I signalling and promote apoptosis in breast cancer cells. *European Journal of Cancer (Oxford, England : 1990), 35*(12), 1717-1723.

Yamada, P. M. & Lee, K. (2009). Perspectives in mammalian IGFBP-3 biology: Local vs. systemic action. *American Journal of Physiology Cell.Physiology, 296*(5), C954-76.

Yamanaka, Y., Fowlkes, J. L., Wilson, E. M., Rosenfeld, R. G. & Oh, Y. (1999). Characterization of insulin-like growth factor binding protein-3 (IGFBP-3) binding to human breast cancer cells: Kinetics of IGFBP-3 binding and identification of receptor binding domain on the IGFBP-3 molecule. *Endocrinology, 140*(3), 1319-1328.

Zehnder, D., Bland, R., Williams, M. C., McNinch, R. W., Howie, A. J., Stewart, P. M. & Hewison, M. (2001). Extrarenal expression of 25-hydroxyvitamin D_3-1α-hydroxylase. *The Journal of Clinical Endocrinology and Metabolism, 86*(2), 888-894.

Zimmermann, E. M., Li, L., Hoyt, E. C., Pucilowska, J. B., Lichtman, S. & Lund, P. K. (2000). Cell-specific localization of insulin-like growth factor binding protein mRNAs in rat liver. *American Journal of Physiology.Gastrointestinal and Liver Physiology, 278*(3), G447-57.

Zinser, G. M. & Welsh, J. (2004). Accelerated mammary gland development during pregnancy and delayed postlactational involution in vitamin D_3 receptor null mice. *Molecular Endocrinology (Baltimore, Md.), 18*(9), 2208-2223.

Zinser, G., Packman, K. & Welsh, J. (2002). Vitamin D_3 receptor ablation alters mammary gland morphogenesis. *Development (Cambridge, England), 129*(13), 3067-3076.